Rigorously computing symmetric stationary states of the Ohta-Kawasaki problem in 3D

Jan Bouwe van den Berg* J.F. Williams†

November 5, 2017

Abstract

In this paper we develop a symmetry preserving method for the rigorous computation of stationary states of the Ohta-Kawasaki partial differential equation in three space dimensions. By preserving the relevant symmetries we achieve an enormous reduction in computational cost. This makes it feasible to construct computer-assisted proofs of complex 3D structures. In particular, we provide the first existence proofs for both the double gyroid and bcc-packed sphere solutions to this problem.

1 Introduction

It is very common for solutions to minimization problems to exhibit (a lot of) symmetries. In this work we construct solutions to an energy minimization problem arising in material science, which possess crystallographic symmetries. In particular, we use rigorously verified numerical methods to find periodic solutions with additional imposed symmetries to the fourth order elliptic partial differential equation (PDE)

$$-\Delta\left(\frac{1}{\gamma^2}\Delta u + u - u^3\right) - (u - m) = 0 \tag{1.1}$$

in three space dimensions. This PDE arises in the Ohta-Kawasaki model for diblock copolymers. The significance of the parameter $m \in [-1, 1]$ and $\gamma > 0$ will be discussed below.

To study solutions of (1.1) which are invariant under a large symmetry group, we develop a rigorous computational framework that incorporates symmetries. By restricting to functions which are invariant under a group action (as well as being periodic) we prove, using computer-assisted analysis, the existence of the double gyroid pattern depicted in Figure 1.1(a), and the body centered cubic (bcc) packed spheres pattern in Figure 1.1(b). Although we focus here on solutions with specific symmetries to a specific PDE, the developed approach is more generally applicable to symmetry-invariant periodic solutions of PDEs.

Before we delve into the mathematics, let us discuss the origin of the Ohta-Kawasaki equation (1.1), sometimes called the diblock copolymer equation.

The physical problem. Diblock copolymers are linear chain molecules consisting of two covalently bonded subchains, type A and type B. The subchains are monomers which repulse each other causing the formation of type A-rich and type B-rich domains. However, the chemical bonding of the subchains means that there cannot be complete macrophase separation (as one finds in the Cahn-Hilliard problem). The combination of the chemical bonding of the chains and the immiscibility of A and B leads to preferred energy configurations where the different types stay "apart but never too far".

*VU Amsterdam, Department of Mathematics, De Boelelaan 1081, 1081 HV Amsterdam, The Netherlands, janbouwe@few.vu.nl; partially supported by NWO-VICI grant 639033109.

†Simon Fraser University, Department of Mathematics, 8888 University Drive Burnaby, BC, V5A 1S6, Canada, jfwillia@sfu.ca.

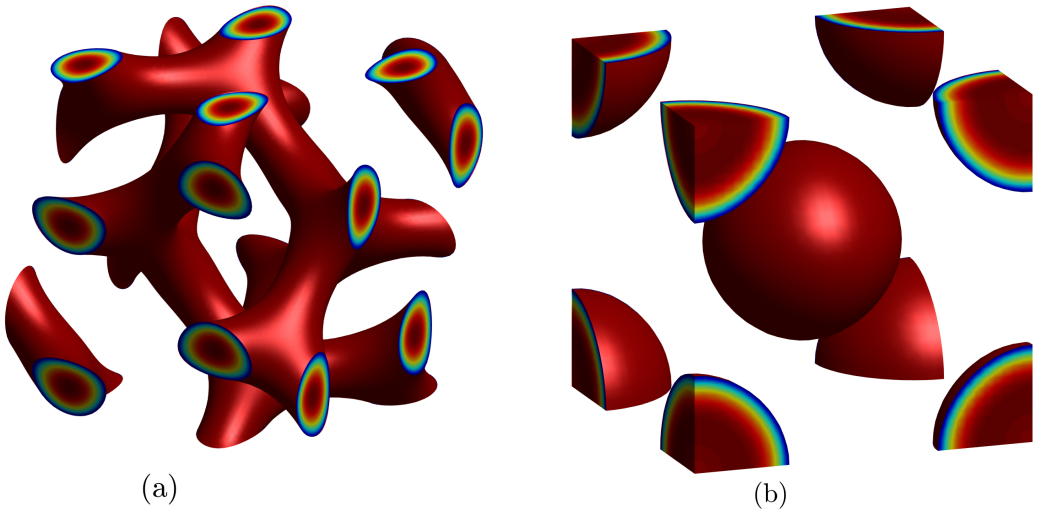

Figure 1.1: Solutions with $m = 0.35$ and $\gamma = 5$ plotted at $u(x, y, z) = -m$. These are both unit cells. The volumes within these levels are type-A dominant. (a) Double gyroid profile. Note there are two disjoint surfaces at the same level. (b) BCC-packed spheres.

Competition between short scale repulsion and long range attraction leads diblock copolymer melts to self-assemble into a rich class of complex structures [2]. This makes the materials exciting from both mathematical and practical points of view. Experimentally, as the temperature and mass ratio are varied, many distinct phases have been observed [15, 1]. We will work under imposed symmetries as *all known phases are periodic and exhibit additional crystallographic symmetries.*

The most commonly seen phases are lamellae, triangularly packed cylinders, bcc packed spheres, double gyroids and close packed spheres. We constructed optimal lamellae and triangularly packed cylinders in [28]; these can be interpreted as essentially 1D stripes and 2D hexagonal spot patterns, respectively. Here we focus on the double gyroid and bcc-packed spheres, since they are the truly three dimensional patterns most widely observed. Furthermore, to our knowledge there is no prior rigorous proof of either phase existing as a solution to (1.1) despite having been seen computationally [21, 7] and experimentally [15].

The mathematical problem. In [17] Ohta and Kawasaki present a free energy functional modelling diblock copolymers, which can be rescaled as

$$E(u) = \frac{1}{|\Omega|} \int_\Omega \frac{1}{2\gamma^2} |\nabla u|^2 + \frac{1}{4}(1-u^2)^2 + \frac{1}{2}|\nabla v|^2 \, dx. \tag{1.2}$$

Since the symmetries of the double gyroid and bcc-packed spheres enforce a cubic unit cell, we consider u to be a periodic function on a cubic domain $\Omega = [0, L]^3$. The average $m = \frac{1}{|\Omega|} \int_\Omega u(x) dx$ determines the ratio between the types A and B subchains. The parameter γ measures the strength of the long range attraction relative to the short range repulsion. The function v is the unique solution of the linear elliptic problem $-\Delta v = u - m$ with periodic boundary conditions and satisfying $\int v = 0$. In the energy (1.2) the first term penalizes jumps in the solution, the second favours $u = \pm 1$ and the last penalizes variation from the mean. Without the final term we have the classical Cahn-Hilliard energy functional which is minimized by configurations which entirely separate into one region where $u = -1$ ("type A") and another where $u = +1$ ("type B"). Critical points of the energy (1.2) are found by taking the gradient in H^{-1} [6], leading to (1.1).

Crystallographic, or space group, symmetries combine the translational symmetries of a lattice

together with other elements such as directional flips, rotation and screw axes. Physically, determining the space group a given material belongs to is an essential step in structure analysis as it minimizes the information required for a complete description. We use this reduction to construct efficient numerical methods which guarantee our solutions have the desired symmetry. The double gyroid and bcc-packed spheres belong to space group 230 and 229, respectively.

We first describe the details of our method for space group 230 and postpone a summary of space group 229 (which is simpler) to Section 3.7. We look for L-periodic solutions

$$u(x_1, x_2, x_3) = u(x_1 + L, x_2, x_3) = u(x_1, x_2 + L, x_3) = u(x_1, x_2, x_3 + L),$$

which are invariant under the actions of space group 230. This group is generated by the transformations

$$S_\sigma x \stackrel{\text{def}}{=} (x_2, x_3, x_1), \tag{1.3a}$$

$$S_\tau x \stackrel{\text{def}}{=} \left(x_2 + \tfrac{L}{4}, x_1 + \tfrac{L}{4}, x_3 + \tfrac{L}{4}\right), \tag{1.3b}$$

$$S_\rho x \stackrel{\text{def}}{=} \left(-x_1, x_2, x_3 + \tfrac{L}{2}\right). \tag{1.3c}$$

We denote the 96 element (symmetry) group generated by $\{S_\sigma, S_\tau, S_\rho\}$ by $\mathcal{G}$. The group includes some elements which are relatively easy to distinguish visibly, such as the half shift along the main diagonal

$$S_\tau^2 x = \left(x_1 + \tfrac{L}{2}, x_2 + \tfrac{L}{2}, x_3 + \tfrac{L}{2}\right),$$

as well as the point symmetry

$$S_\pi x \stackrel{\text{def}}{=} (L - x_1, L - x_2, L - x_3). \tag{1.4}$$

Definition 1.1. *An L-periodic function u is said to be $\mathcal{G}$-symmetric if $u(Sx) = u(x)$ for all $S \in \mathcal{G}$.*

To prove the existence of a $\mathcal{G}$-symmetric solution representing a double gyroid pattern, as depicted in Figure 1.1(a), we build on previously developed rigorous computational methods, see [22, 25] and the references therein. This technique is based on the Banach fixed point theorem, where the conditions for proving a contraction are reduced to checking a single, explicit but complicated, inequality, which can be accomplished with the assistance of a computer. The main contribution of this paper is the development of a flexible symmetry framework in such a rigorous numerics setting. Preserving all symmetries is not only imperative for the physical problem, but also makes our method very efficient computationally as we reduce the number of coefficients we need to store and compute on by a factor of approximately 100. This makes it feasible to prove the existence of complicated (but symmetric) solutions of the PDE (1.1) in three space dimensions, see Section 4 for specific results.

Previous results. Most relevant to the current work are results discussing the structure of solutions near the point $m = 0, \gamma = 2$ such as [6, 4, 28]. Various solutions have been investigated, with periodic minimizers found as $\gamma \to \infty$ [5, 12]. There have also been considerable numerical investigations of this problem by integrating the PDE in time [6, 21] or directly solving the stationary problem [20] amongst others.

This paper is, in some ways, an extension of the ideas of [28] to three dimensions. That is, we use a similar problem formulation and similar tools from rigorous numerics to ensure that our computed "numerical solutions" (finite approximations) are close to solutions to the full infinite dimensional problem in a precise and rigorously verified manner. Wanner and colleagues have used rigorous numerics on this problem in one space dimension both to construct solutions [29] and to find and continue bifurcation points [16].

Outline of paper. In this paper we prove existence of solutions to (1.1) whilst imposing symmetries observed in experimentally discovered profiles. Our method of proof requires the construction of abstract functional analytic bounds which are then implemented practically and verified numerically about given approximate solutions. The details of the approach we use for rigorous numerics

and the various required general estimates are laid out in Section 2. In Section 3 we explain the symmetry group, how to encode it into our estimates and how to preserve it computationally. Section 4 contains rigorously verified solutions to (1.1) from space groups 229 and 230, discusses some of the numerical and algorithmic issues, and also presents some rather unusual profiles. Finally, in Section 5, we discuss possible further extensions of this approach.

Code to generate the figures in this paper and run the proofs is available at [27].

2 Rigorous computational setup

We use a functional analytic approach to rigorous numerics. The crux of this methodology is to perform validated computations to verify that an appropriate fixed point operator is contracting in a neighbourhood of our finite dimensional approximation. Before constructing the fixed point theorem we need to formulate our problem and detail the necessary norms and spaces. This builds on earlier work in two [11, 9, 28, 3] and higher [10] dimensional problems. For clarity of exposition, we start with the setup and estimates without assuming a symmetric setting. The modifications needed to incorporate the symmetries will be discussed in Sections 3.3–3.6.

2.1 Problem formulation

We set $\ell \stackrel{\text{def}}{=} \frac{L}{2\pi}$. Looking for a periodic solution, we write

$$u(x) = \sum_{k\in\mathbb{Z}^3} c_k e^{ik\cdot x/\ell},$$

with $c_0 = m$. This transforms the differential equation (1.1) into Fourier space:

$$h_k(c) \stackrel{\text{def}}{=} (\gamma^{-2}\ell^{-4}\mathbf{k}^4 - \ell^{-2}\mathbf{k}^2 + m)c_k + \ell^{-2}\mathbf{k}^2\langle c^3\rangle_k = 0, \tag{2.1}$$

for $k \in \mathbb{Z}^3_0 \stackrel{\text{def}}{=} \mathbb{Z}^3 \setminus \{0\}$, where

$$\mathbf{k} \stackrel{\text{def}}{=} \left(|k_1|^2 + |k_2|^2 + |k_3|^2\right)^{1/2}.$$

We note that

$$h_0 \stackrel{\text{def}}{=} c_0 - m \tag{2.2}$$

vanishes, since we impose $c_0 = m$. Finally, $\langle\cdot\cdot\rangle$ denotes the discrete convolution product in three dimensions:

$$\langle a\, b\rangle_k \stackrel{\text{def}}{=} \sum_{k'\in\mathbb{Z}^3} a_{k'} b_{k-k'}, \tag{2.3}$$

which generalizes to $\langle c^3\rangle = \langle\langle c\, c\rangle\, c\rangle$.

2.2 Functional analytic setup

We will use the 1-norm in Fourier space:

$$\|c\| \stackrel{\text{def}}{=} \sum_{k\in\mathbb{Z}^3} |c_k|. \tag{2.4}$$

The corresponding Banach space is

$$X \stackrel{\text{def}}{=} \{(c_k)_{k\in\mathbb{Z}^3} \,:\, c_k \in \mathbb{C}\,,\, \|c\| < \infty\}. \tag{2.5}$$

We are interested in real-valued u only, and one may be tempted to require $c_{-k} = c_k^*$ in the definition of X. However, this is just one of the symmetries that the solutions considered in this paper will have, and we will deal with all these symmetries in Section 3 in a integrated fashion.

It is convenient to introduce the basis vectors e_k:

$$(\mathrm{e}_k)_{k'} = \begin{cases} 1 & \text{for } k = k' \\ 0 & \text{for } k \neq k'. \end{cases}$$

The solution average, $c_0 = m$, is fixed, hence we look for zeros of $(h_k)_{k\in\mathbb{Z}^3_0}$ as defined in (2.1) in the affine space

$$X_m \stackrel{\text{def}}{=} \{c \in X \,:\, c_0 = m\}. \tag{2.6}$$

Since X_m is an affine linear space, it is more convenient to shift the problem to the linear space

$$X_0 \stackrel{\text{def}}{=} \{c \in X \,:\, c_0 = 0\}$$

as follows. Any element $\tilde{c} \in X_m$ can be written as $\tilde{c} = m\mathrm{e}_0 + c$, with $c \in X_0$. Instead of h with domain X_m we now consider f with domain X_0 defined by

$$f_k(c) \stackrel{\text{def}}{=} h_k(m\mathrm{e}_0 + c). \tag{2.7}$$

Without loss of generality, elements in X_0 may be indexed by $k \in \mathbb{Z}^3_0$ rather than $k \in \mathbb{Z}^3$, and the norm on X_0 is given by

$$\|c\| = \sum_{k\in\mathbb{Z}^3_0} |c_k|.$$

The norm (2.4) on X has the Banach algebra property

$$\|\langle a\, b\rangle\| \leq \|a\|\|b\| \qquad \text{for all } a, b \in X.$$

We note that the convolution of two elements of X_0 lies in X but not necessarily in X_0. The second convenient property of the 1-norm (2.4) is that the dual of X_0 is the corresponding l^∞ space:

$$X_0^* = \Big\{(d_k)_{k\in\mathbb{Z}^3_0} \,:\, \sup_{k\in\mathbb{Z}^3_0} |d_k| < \infty\Big\}.$$

Any bounded linear operator Γ on X_0 can be characterized by $\Gamma_{kk'} = (\Gamma \mathrm{e}_{k'})_k$ with $k, k' \in \mathbb{Z}^3_0$. It readily follows that the operator norm of Γ is given by

$$\|\Gamma\|_{B(X_0)} = \sup_{k'\in\mathbb{Z}^3_0} \|\Gamma \mathrm{e}_{k'}\| \tag{2.8}$$

$$= \sup_{k'\in\mathbb{Z}^3_0} \sum_{k\in\mathbb{Z}^3_0} |\Gamma_{kk'}|. \tag{2.9}$$

We will compute in a finite dimensional subspace. Let $K \in \mathbb{N}$, and let

$$N = N(K) \stackrel{\text{def}}{=} \big|\{k \in \mathbb{Z}^3 \,:\, 0 < \mathbf{k} \leq K\}\big|. \tag{2.10}$$

where $|.|$ denotes the number of elements in the set. We define

$$X_N \stackrel{\text{def}}{=} \{c \in X_0 \,:\, c_k = 0 \text{ for all } \mathbf{k} > K\}. \tag{2.11}$$

Clearly, X_N can be identified with a finite dimensional space $\mathbb{C}^N$, and we will implicitly use this identification whenever convenient. Elements of $X_N \cong \mathbb{C}^N$ are sometimes denoted by c_N. The natural complement of X_N is

$$X_\infty \stackrel{\text{def}}{=} \{c \in X \,:\, c_k = 0 \text{ for all } \mathbf{k} \leq K\}.$$

The projections onto X_N and X_∞ will be denoted by π_N and π_∞, respectively.

In preparation for a computer-assisted proof, we first find numerically an approximate zero $\bar{c}$ in X_N of the Galerkin projection $\pi_N f$, i.e.

$$\bar{c} \in X_N \cong \mathbb{C}^N \text{ such that } \pi_N f(\bar{c}) \approx 0.$$

We also compute an $N \times N$ matrix A_N, namely a numerical (i.e. not exact) inverse of the Jacobian J_N of the finite dimensional map $c_N \to \pi_N f(c_N)$ evaluated at $c_N = \bar{c}$.

With f defined in (2.7) we now introduce the fixed point operator on X_0 as

$$T(c) \stackrel{\text{def}}{=} c - Af(c).$$

Here A is a linear block-diagonal operator of the form

$$\pi_N Ac = A_N \pi_N c, \tag{2.12a}$$

$$\pi_\infty Ac = \Lambda^{-1} \pi_\infty, \tag{2.12b}$$

and Λ is the diagonal operator given by

$$(\Lambda c)_k \stackrel{\text{def}}{=} \lambda_k c_k,$$

where

$$\lambda_k \stackrel{\text{def}}{=} \gamma^{-2}\ell^{-4}\mathbf{k}^4 - \ell^{-2}\mathbf{k}^2 + m.$$

We assume that $K \in \mathbb{N}$ is sufficiently large, say $K \geq \gamma\ell$, so that $\lambda_k \neq 0$ for all $\mathbf{k} > K$.

Provided A is injective (this will follow from the assumptions in Theorem 2.1, see its proof), the zero finding problem $f(c) = 0$ is now equivalent to the fixed point problem $T(c) = c$. Since A is an approximation of the inverse of the Jacobian of f at $\bar{c}$, one may expect T to be a contraction mapping on small balls around $\bar{c}$. We denote by B the unit ball in X_0:

$$B = \{(v_k)_{k \in \mathbb{Z}^3_0} \,:\, \|v\| \leq 1\}.$$

In Subsections 2.3 and 2.4 we will derive explicit expressions for $Y > 0$ and $Z : \mathbb{R}^+ \to \mathbb{R}^+$, which provide bounds on the residue and the derivative, respectively:

$$\|T(\bar{c}) - \bar{c}\| \leq Y, \tag{2.13}$$

$$\sup_{w,v \in B} \|DT(\bar{c} + rw)v\| \leq Z(r). \tag{2.14}$$

The key mathematical step is the next lemma which shows that it suffices to check that

$$Y + \tilde{r}Z(\tilde{r}) - \tilde{r} < 0, \tag{2.15}$$

for some $\tilde{r} > 0$, to conclude that there is a unique solution of $f(c) = 0$ in the ball of radius $\tilde{r}$ around the numerical guess $\bar{c}$. Since $Z(r)$, as obtained in Section 2.4, is a second order polynomial, the left-hand side of (2.15) is often called the radii polynomial (a cubic one in this case) in the literature, see e.g. [8, 24].

Theorem 2.1. *Let $K \geq \gamma\ell$. Assume that Y and $Z(r)$ satisfy the bounds* (2.13) *and* (2.14). *Let $\tilde{r} > 0$ be such that the inequality* (2.15) *is satisfied. Then f has a unique zero $\widehat{c}$ in*

$$B_{\tilde{r}}(\bar{c}) \stackrel{\text{def}}{=} \{c \in X_0 \,:\, \|c - \bar{c}\| \leq \tilde{r}\}. \tag{2.16}$$

Proof. It is straightforward to check that the bounds (2.13) and (2.14) together with (2.15) imply that T is a contraction mapping on $B_{\tilde{r}}(\bar{c})$, see e.g. [8] for more details. By the Banach contraction theorem, this implies that T has a unique fixed point $\widehat{c}$ in $B_{\tilde{r}}(\bar{c})$. To conclude that $f(\widehat{c}) = 0$ we need to establish that A is injective. First, $\pi_\infty A$ is injective on X_∞ since $\lambda_k^{-1} > 0$ for $\mathbf{k} > K \geq \gamma\ell$, hence it suffices to prove that the matrix A_N is injective (or equivalently, invertible). We observe that $Z(\tilde{r}) < 1$ by (2.15). Let $0 \neq v_N \in X_N$ be arbitrary. On the one hand the bound (2.14) implies that

$$\|\pi_N DT(\bar{c})v_N\| \leq Z(\tilde{r})\|v_N\| < \|v_N\|, \tag{2.17}$$

while on the other hand

$$\pi_N DT(\bar{c})v_N = (I_N - A_N J_N)v_N, \tag{2.18}$$

where J_N is the Jacobian of the finite dimensional map $c_N \to \pi_N f(c_N)$ at $c_N = \bar{c}$, and I_N denotes the identity matrix acting on X_N. By combining (2.17) and (2.18) it follows that A_N is invertible, hence injective. □

Remark 2.2 (Error estimate)**.** *Our approach gives a precise and computable error bound. Let*

$$\overline{u}(x) \stackrel{\text{def}}{=} m + \sum_{0<\mathbf{k}\le K} \overline{c}_k e^{ik\cdot x/\ell}$$
$$\widehat{u}(x) \stackrel{\text{def}}{=} m + \sum_{\mathbf{k}\in\mathbb{Z}^3_0} \widehat{c}_k e^{ik\cdot x/\ell}. \tag{2.19}$$

It follows from the definition of the 1*-norm on* X *and the observation that* $\widehat{c}$ *lies in* $B_{\tilde{r}}(\overline{c})$ *as defined in* (2.16)*, that the* C^0 *error between the numerical approximation* $\overline{u}$ *and the (true) solution* $\widehat{u}$ *of* (1.1) *is bounded by* $\tilde{r}$*:*

$$\|\widehat{u} - \overline{u}\|_\infty \le \|\widehat{c} - \overline{c}\| \le \tilde{r}.$$

Remark 2.3 (Real-valuedness)**.** *It is not a priori clear that the solution* $\widehat{u}(x)$ *defined in* (2.19) *is real-valued. One way to obtain a real-valued solution is by using the equivariance of* f *with respect to the operator* $\gamma_0 : X_0 \to X_0$ *given by* $(\gamma_0 c)_k = c^*_{-k}$*. Indeed, it is not difficult to check that*

$$f(\gamma_0 c) = \gamma_0 f(c).$$

If we choose a symmetric numerical approximation $\overline{c}$*, i.e.* $\gamma_0\overline{c} = \overline{c}$ *(hence* $\overline{u}(x)$ *is real-valued), then the ball* $B_{\tilde{r}}(\overline{c})$ *is invariant under* γ_0*, and it readily follows from the uniqueness of the zero of* f *in* $B_{\tilde{r}}(\overline{c})$ *that* $\gamma_0\widehat{c} = \widehat{c}$*, hence* $\widehat{u}(x)$ *is real-valued. In the current paper we will not use this argument. Instead, all symmetries (among which* $u(x) = u(x)^*$*) will be dealt with in a unified manner in Section 3 by reducing the number of variables. We note that this equivariance argument is not specific to complex conjugation and can be used for other symmetries as well.*

Remark 2.4 (Smoothness)**.** *Since the Fourier coefficients* $\widehat{c} \in X_0$ *are summable, the solution* $\widehat{u}(x)$ *is continuous. Moreover, it follows from* (2.1) *and* (2.7) *and the Banach algebra property that any zero* $\widehat{c}$ *of* f *satisfies* $(\mathbf{k}^2\widehat{c}_k) \in X_0$*, and by bootstrapping* $(\mathbf{k}^n\widehat{c}_k) \in X_0$ *for any* $n \in \mathbb{N}$*. Hence we obtain that* $\widehat{u}(x) \in C^\infty$*. Alternatively, we could have set up the problem with an exponentially weighted norm* $\|c\|_\xi = \sum_{k\in\mathbb{Z}^3} |c_k|\xi^{\mathbf{k}}$*, with* $\xi > 1$*, as to recover* analyticity *of the solution, see e.g. [13, 28]. This presents no technical obstacle, but in the current paper we avoid this slight notational burden for simplicity of presentation.*

2.3 The bound Y

We derive a bound satisfying (2.13). We recall that $\overline{c}_k = 0$ for $\mathbf{k} > K$ and note that

$$[T(\overline{c}) - \overline{c}]_k = [-Af(\overline{c})]_k = \begin{cases} [A_N \pi_N f(\overline{c})]_k & \text{for } 0 < \mathbf{k} \le K \\ \frac{1}{\lambda_k} f(\overline{c})_k & \text{for } K < \mathbf{k} \le 3K \\ 0 & \text{for } \mathbf{k} > 3K, \end{cases}$$

since for $\mathbf{k} > K$ we have

$$f(\overline{c})_k = \ell^{-2}\mathbf{k}^2 \langle (m\mathrm{e}_0 + \overline{c})^3 \rangle_k,$$

which vanishes for $\mathbf{k} > 3K$. Hence, there are only finitely many nonzero terms in $Af(\overline{c})$, which can all be computed with interval arithmetic. We thus obtain a bound of the type (2.13) by setting

$$Y = \uparrow \sum_{0<\mathbf{k}\le 3K} \big|[Af(\overline{c})]_k\big|,$$

where by $\uparrow I$ we indicate the maximum of the interval I obtained from an interval arithmetic computation.

2.4 The bound Z

To derive a bound satisfying (2.14), we start by calculating the derivative

$$Df_k(c)v = \lambda_k v_k + 3\ell^{-2}\mathbf{k}^2\langle (m\mathrm{e}_0 + c)^2 v\rangle_k.$$

Hence, using the shift property of the convolution

$$\langle c\mathrm{e}_{k'}\rangle_k = c_{k-k'}, \tag{2.20}$$

we can express the components of the Jacobian as

$$Df_k(c)\mathrm{e}_{k'} = \delta_{kk'}\lambda_k + 3\ell^{-2}\mathbf{k}^2\langle (m\mathrm{e}_0 + c)^2\rangle_{k-k'}, \tag{2.21}$$

where δ denotes the Kronecker delta. Next we decompose

$$Df(\overline{c} + rw) = J + [Df(\overline{c}) - J] + [Df(\overline{c} + rw) - Df(\overline{c})]\,,$$

where J is an approximate Jacobian defined by

$$\pi_N Jc = J_N \pi_N c, \tag{2.22a}$$
$$\pi_\infty Jc = \Lambda \pi_\infty c. \tag{2.22b}$$

We recall that J_N is the *exact* Jacobian of the finite dimensional map $c_N \to \pi_N f_N(c_N)$ evaluated at $c_N = \overline{c}$, i.e. $J_N\pi_N v = \pi_N Df(\overline{c})\pi_N v$, or equivalently

$$(J\mathrm{e}_{k'})_k = (DF(\overline{c})\mathrm{e}_{k'})_k \qquad \text{for } \mathbf{k}, \mathbf{k}' \le K. \tag{2.23}$$

In this notation we may split $DT(\overline{c} + rw)v$ as follows:

$$DT(\overline{c} + rw)v = [I - ADf(\overline{c} + rw)]v = \big[I - AJ\big]v - A\big[Df(\overline{c}) - J\big]v - A\big[Df(\overline{c} + rw) - Df(\overline{c})\big]v.$$

We aim to obtain bounds on the three terms

$$\begin{aligned} Q_1 &\ge \sup_{v\in B} \|[I - AJ]v\| \\ Q_2 &\ge \sup_{v\in B} \|A[Df(\overline{c}) - J]v\| \\ Q_3 &\ge \sup_{v,w\in B} \|A[Df(\overline{c} + rw) - Df(\overline{c})]v\| \end{aligned}$$

separately. Here Q_3 will depend (quadratically) on r.

The bound Q_1 is a bound on the operator norm (given by (2.9)) of $I - AJ$. We note that, by (2.12) and (2.22),

$$\begin{aligned} \pi_N[I - AJ]v &= [I_N - A_N J_N]\pi_N v, \\ \pi_\infty[I - AJ]v &= 0\,. \end{aligned}$$

Evaluating $\|I - AJ\|_{B(X_0)}$ is thus a finite computation, since the only non-vanishing elements $([I - AJ]\mathrm{e}_{k'})_k$ are those with $0 < \mathbf{k}, \mathbf{k}' \le K$. In other words, the bound Q_1 is the operator 1-norm of the matrix $I_N - A_N J_N$ (i.e. (2.9) restricted to a finite set of indices), computed using interval arithmetic:

$$Q_1 = \uparrow\|I_N - A_N J_N\|_1.$$

The bound Q_2 is a bound on the operator norm of $A[Df(\overline{c}) - J]$. We start with

$$([Df(\overline{c}) - J]v)_k = \begin{cases} 3\ell^{-2}\mathbf{k}^2\langle (m\mathrm{e}_0 + \overline{c})^2\pi_\infty v\rangle_k & \text{for } 0 < \mathbf{k} \le K \\ 3\ell^{-2}\mathbf{k}^2\langle (m\mathrm{e}_0 + \overline{c})^2 v\rangle_k & \text{for } \mathbf{k} > K. \end{cases} \tag{2.24}$$

Only the convolution term appears, since the linear term cancels, and it follows from (2.23) that for $\mathbf{k} \le K$ the terms that depend on $\pi_N v$ vanish. We use the expression (2.8) for the operator norm and split the estimate in $\mathbf{k}' \le 3K$ and $\mathbf{k}' > 3K$. Starting with the tail terms, we infer from (2.24) and (2.20) that

$$([Df(\overline{c}) - J]\mathrm{e}_{k'})_k = 0 \qquad \text{for } \mathbf{k}' > 3K \text{ and } \mathbf{k} \le K. \tag{2.25}$$

Furthermore, for $\mathbf{k}' > 3K$ and $\mathbf{k} > K$ we have

$$(A[Df(\overline{c}) - J]\mathrm{e}_{k'})_k = (\Lambda^{-1}\pi_\infty[Df(\overline{c}) - J]\mathrm{e}_{k'})_k = \frac{3\ell^{-2}\mathbf{k}^2}{\lambda_k}\langle(m\mathrm{e}_0 + \overline{c})^2\rangle_{k-k'}.$$

We estimate

$$\frac{\ell^{-2}\mathbf{k}^2}{\gamma^{-2}\ell^{-4}\mathbf{k}^4 - \ell^{-2}\mathbf{k}^2 + 1} \le C_K \stackrel{\text{def}}{=} \frac{\ell^{-2}K^2}{\gamma^{-2}\ell^{-4}K^4 - \ell^{-2}K^2 + 1} \tag{2.26}$$

for all $\mathbf{k} > K$, where we have assumed that $K \ge \ell \max\{\gamma, \gamma^{1/2}\}$ (in practice this is a very mild restriction).

We now obtain the tail estimate

$$\|A[Df(\overline{c}) - J]\mathrm{e}_{k'}\| \le 3C_K\|\langle(m\mathrm{e}_0 + \overline{c})^2\rangle\| \qquad \text{for all } \mathbf{k}' > 3K.$$

For $\mathbf{k}' \le 3K$ we infer from (2.24) and (2.20) that $(A[Df(\overline{c}) - J]\mathrm{e}_{k'})_k$ vanishes for $\mathbf{k} > 5K$. Hence it takes a finite computation using interval arithmetic to evaluate

$$\widetilde{Q}_2 = \uparrow \max_{0<\mathbf{k}'\le 3K} \|A[Df(\overline{c}) - J]\mathrm{e}_{k'}\|,$$

exploiting (2.20), (2.23) and (2.25) for efficiency in practice. We thus obtain the bound

$$Q_2 = \max\{\widetilde{Q}_2, \uparrow 3C_K\|\langle(m\mathrm{e}_0 + \overline{c})^2\rangle\|\}.$$

We evaluate the third term by expanding

$$([Df(\overline{c} + rw) - Df(\overline{c})]v)_k = 6\ell^{-2}\mathbf{k}^2\langle(m\mathrm{e}_0 + \overline{c})wv\rangle_k r + 3\ell^{-2}\mathbf{k}^2\langle w^2 v\rangle_k r^2, \tag{2.27}$$

and we estimate the linear and quadratic terms in r separately. Hence we define, for $k \in \mathbb{Z}^3_0$,

$$P(v,w)_k \stackrel{\text{def}}{=} 6\ell^{-2}\mathbf{k}^2\langle(m\mathrm{e}_0 + \overline{c})wv\rangle_k,$$
$$R(v,w)_k \stackrel{\text{def}}{=} 3\ell^{-2}\mathbf{k}^2\langle w^2 v\rangle_k,$$

and we aim to obtain bounds

$$Q_{3,1} \ge \sup_{v,w\in B} \|AP(v,w)\|,$$
$$Q_{3,2} \ge \sup_{v,w\in B} \|AR(v,w)\|.$$

We must be careful with the linear term, as while $\langle wv\rangle$ lies in X and $\|\langle wv\rangle\| \le \|w\|\|v\| \le 1$ for $v, w \in B$, the convolution product $\langle wv\rangle$ does not necessarily lie in X_0. We interpret $\langle(m\mathrm{e}_0+\overline{c})wv\rangle = \langle(m\mathrm{e}_0 + \overline{c})\langle wv\rangle\rangle$ and we want to "replace" the two arbitrary elements $v, w \in X_0$ with $\|v\|, \|w\| \le 1$ by an arbitrary element $q \in X$ with $\|q\| \le 1$. To this end we introduce, for $k \in \mathbb{Z}^3_0$,

$$(\widetilde{P}q)_k \stackrel{\text{def}}{=} 6\ell^{-2}\mathbf{k}^2\langle(m\mathrm{e}_0 + \overline{c})q\rangle_k,$$

which may be viewed as a linear operator from X to X_0. As explained above, we then have the estimate

$$\sup_{v,w\in B} \|AP(v,w)\| \le \sup_{q\in X, \|q\|\le 1} \|A\widetilde{P}q\|. \tag{2.28}$$

We interpret $A\widetilde{P}$ in the right-hand side of (2.28) as a linear operator which maps X to X_0, and we estimate its norm analogously to the estimate above for $A[Df(\bar{c})-J]$. It takes a finite computation using interval arithmetic to evaluate

$$\widetilde{Q}_{3,1} = \uparrow \max_{0\le \mathbf{k}'\le 2K} \|A\widetilde{P}\mathrm{e}_{k'}\|,$$

where $k'=0$ is included in the maximum. In particular, for all $\mathbf{k}' \le 2K$ we have that $(A\widetilde{P}\mathrm{e}_{k'})_k$ vanishes for $\mathbf{k} > 3K$. Estimating the tail term as before, we obtain the bound

$$Q_{3,1} = \max\{\widetilde{Q}_{3,1}, \uparrow 6C_K\|m\mathrm{e}_0 + \bar{c}\|\}$$

on the operator norm of $A\widetilde{P}$ and thus, via (2.28), on $\|AP(v,w)\|$, as desired.

Finally, we deal with the quadratic term in (2.27). Analogous to the arguments above leading to the bound $Q_{3,1}$, we introduce, for $k \in \mathbb{Z}^3_0$,

$$(\widetilde{R}q)_k \stackrel{\text{def}}{=} 3\ell^{-2}\mathbf{k}^2 q_k,$$

which we view as a diagonal linear operator from X to X_0 (or from X_0 to X_0, as $\widetilde{R}\mathrm{e}_0 = 0$). It takes a finite computation using interval arithmetic to evaluate

$$\widetilde{Q}_{3,2} = \uparrow \max_{0<\mathbf{k}'\le K} \|A\widetilde{R}\mathrm{e}_{k'}\|,$$

which is in fact just the 1-norm of the matrix $A_N\pi_N\widetilde{R}\pi_N$. Estimating the tail term as before, we obtain the bound

$$Q_{3,2} = \max\{\widetilde{Q}_{3,2}, \uparrow 3C_K\}$$

on the operator norm of $A\widetilde{R}$ and thus on $\|AR(v,w)\|$, as desired.

By collecting terms we find that

$$Z(r) = Q_1 + Q_2 + rQ_{3,1} + r^2Q_{3,2}$$

gives a bound satisfying (2.14).

3 Symmetry preserving formulation

3.1 Representation of the symmetry group in Fourier space

We recall from Section 2.1 that we set $\ell \stackrel{\text{def}}{=} \frac{L}{2\pi}$, and write the Fourier transform of an L-periodic function as

$$u(x) = \sum_{k\in\mathbb{Z}^3} c_k e^{ik\cdot x/\ell}.$$

In this section we consider the symmetry group $\widehat{G}$ generated by transforming the spatial symmetries $\mathcal{G}$ to Fourier space *and* complex conjugation of the u variable (thus incorporating that we are only interested in real-valued u). For any $S \in \mathcal{G}$ we obtain a corresponding *right* group action γ_S satisfying

$$u(Sx) = \sum_{k\in\mathbb{Z}^3} [\gamma_S c]_k e^{ik\cdot x/\ell} \qquad \text{for } S \in \mathcal{G}. \tag{3.1}$$

In particular, for the generators $\{S_\sigma, S_\tau, S_\rho\}$ of $\mathcal{G}$ the corresponding group actions γ on Fourier space are given by

$$[\gamma_{S_\sigma} c]_{k_1,k_2,k_3} = c_{k_2,k_3,k_1}, \tag{3.2a}$$

$$[\gamma_{S_\tau} c]_{k_1,k_2,k_3} = e^{i\pi(k_1+k_2+k_3)/2} c_{k_2,k_1,k_3}, \tag{3.2b}$$

$$[\gamma_{S_\rho} c]_{k_1,k_2,k_3} = e^{i\pi k_3} c_{-k_1,k_2,k_3}. \tag{3.2c}$$

For the other elements $S \in \mathcal{G}$ the corresponding group action γ_S acting on c is obtain by transitivity, see Remark 3.1. For example, for the point symmetry S_π in (1.4) we obtain

$$[\gamma_{S_\pi} c]_{k_1,k_2,k_3} = e^{i\pi(k_1+k_2+k_3)} c_{k_1,k_2,k_3}.$$

Remark 3.1. *To be explicit, if $S \in \mathcal{G}$ is represented by $Sx = Ax + bL$, with A a unitary matrix and b a vector with values in $[0,1]$, then $[\gamma_S c]_k = e^{2\pi i k \cdot A^{-1} b} c_{Ak}$. Furthermore, for $S_1, S_2 \in \mathcal{G}$, let us denote $u_1(x) = u(S_1 x)$ and $u_{12} = u(S_1 S_2 x) = u_1(S_2 x)$. When u has Fourier coefficients c, then u_1 has Fourier coefficients $\gamma_{S_1} c$ by* (3.1)*, and u_{12} has Fourier coefficients $\gamma_{S_2}\gamma_{S_1} c$ again by* (3.1)*. Hence γ_S is a* right *group action:*

$$\gamma_{S_1 S_2} c = \gamma_{S_2}\gamma_{S_1} c.$$

In addition to the group (action of) $\mathcal{G}$, we take into account the symmetry coming from complex conjugation of u, which is represented in Fourier space by the transformation

$$[\gamma_0 c]_{k_1,k_2,k_3} \stackrel{\text{def}}{=} c^*_{-k_1,-k_2,-k_3}\,. \tag{3.3}$$

Rather than working with γ_0 directly, it is more convenient to consider the composition of γ_0 and γ_{S_π}, which we denote by γ_*:

$$[\gamma_* c]_k \stackrel{\text{def}}{=} c^*_k\,.$$

The full symmetry group $\widehat{G}$ under consideration is generated by $\{\gamma_{S_\sigma}, \gamma_{S_\tau}, \gamma_{S_\rho}, \gamma_*\}$. Here we have slightly abused notation by identifying the action γ with the group itself (since γ is a faithful action/representation of $\mathcal{G}$). The group $\widehat{G}$ has 192 elements. It splits into two normal subgroups: $\widehat{G} = G \times H$. Here $H \stackrel{\text{def}}{=} \{e, \gamma_*\}$, where e denotes the identity, and G is the subgroup generated by $\{\gamma_{S_\sigma}, \gamma_{S_\tau}, \gamma_{S_\rho}\}$. Obviously $G \cong \mathcal{G}$.

3.2 Reduction to symmetry variables

From now on we will denote elements of G by g, and the action of G on c by $\gamma_g c$. The set of Fourier coefficient that are symmetry invariant under G is given by

$$X^{\text{sym}} \stackrel{\text{def}}{=} \{c \in X \,:\, \gamma_g c = c \text{ for all } g \in G\}.$$

Lemma 3.2. *Let $c \in X^{\text{sym}}$ with $c_k \in \mathbb{R}$ for all $k \in \mathbb{Z}^3$. Then $u(x) = \sum_{k\in\mathbb{Z}^3} c_k e^{ik\cdot x/\ell}$ is real-valued and $\mathcal{G}$-symmetric in the sense of Definition 1.1.*

Proof. Since c is invariant under the action of G it follows from (3.1) that u is invariant under the symmetries generated by (1.3) (in the sense of Definition 1.1). The assumption that c is real-valued implies that c is also invariant under H, hence under the full symmetry group $\widehat{G}$. It follows from (3.3) that $u(x)$ is real-valued (since $\gamma_0 \in \widehat{G}$). □

Remark 3.3. *The subgroup H is somewhat particular to the symmetries which define the space groups 229 and 230, that we consider in this paper. It implies that we may restrict attention to* real-valued *Fourier coefficients. Although this is convenient from a computational point of view, it is not essential. In Remark 2.3 we explained how to recover real-valuedness of $u(x)$ by using equivariance of f under complex conjugation (rather than invariance of c under H). The remainder of the analysis deals with G only, and we consider the general case of complex-valued Fourier coefficients.*

We now study the group action of G in more detail. We write the *right* action γ_g of $g \in G$ on $c \in X$ as

$$(\gamma_g c)_k = \alpha_g(k)\, c_{\beta_g(k)}.$$

Here β_g is itself a *left* group action on $\mathbb{Z}^3$, i.e.,

$$\beta_{g_1 g_2}(k) = \beta_{g_1}(\beta_{g_2}(k)), \tag{3.4}$$

whereas $\alpha_g(k) \in \{z \in \mathbb{C} : |z| = 1\}$ for all $k \in \mathbb{Z}^3$. The formulas for α_g and β_g for the generators can be read off from (3.2). The product structure on α is given by

$$\alpha_{g_1 g_2}(k) = \alpha_{g_1}(\beta_{g_2} k)\alpha_{g_2}(k), \tag{3.5}$$

which follows directly from $\gamma_{g_1 g_2} = \gamma_{g_2}\gamma_{g_1}$.

Lemma 3.4. *The space X^{sym} is closed under the convolution product* (2.3).

Proof. We first note that $\alpha_g(k+k') = \alpha_g(k)\alpha_g(k')$ and $\alpha_g(0) = 1$ for all $g \in G$. Furthermore, $\beta_g(k+k') = \beta_g(k) + \beta_g(k')$. By using that β_g permutes $\mathbb{Z}^3$ we obtain

$$\begin{aligned}
\langle \gamma_g a, \gamma_g b\rangle_k &= \sum_{k'\in\mathbb{Z}^3} \alpha_g(k')a_{\beta_g(k')}\,\alpha_g(k-k')b_{\beta_g(k-k')} \\
&= \alpha_g(k)\sum_{k'\in\mathbb{Z}^3} \alpha_g(k')\alpha_g(k)\alpha_g(-k')\,a_{\beta_g(k')}b_{\beta_g(k)-\beta_g(k')} \\
&= \alpha_g(k)\sum_{k''\in\mathbb{Z}^3} \alpha_{k''}b_{\beta_g(k)-k''} \\
&= (\gamma_g\langle ab\rangle)_k\,.
\end{aligned}$$

This concludes the proof. □

We now list some properties of α that will be useful in what follows.

Lemma 3.5. *Let $k \in \mathbb{Z}^3$ and $g, h \in G$.*

(a) $\alpha_g(k)\,\alpha_{g^{-1}}(\beta_g(k)) = 1$.

(b) *If $\beta_g(k) = \beta_h(k)$ and $\alpha_{h^{-1}g}(k) = 1$, then $\alpha_g(k) = \alpha_h(k)$.*

(c) *If $\beta_g(k) = k$, then $\alpha_{hgh^{-1}}(\beta_h(k)) = \alpha_g(k)$.*

Proof. For part (a) we use (3.5) to infer that

$$1 = \alpha_e(k) = \alpha_{g^{-1}g}(k) = \alpha_{g^{-1}}(\beta_g(k))\,\alpha_g(k).$$

For part (b) we write $g = hh^{-1}g$. From the first assumption and (3.4) if follows that $\beta_{h^{-1}g}(k) = k$. By applying (3.5) to $g_1 = h$ and $g_2 = h^{-1}g$, we see that the second assumption implies

$$\alpha_g(k) = \alpha_{hh^{-1}g}(k) = \alpha_h(\beta_{h^{-1}g}(k))\,\alpha_{h^{-1}g}(k) = \alpha_h(k).$$

For part (c) we write $k' = \beta_h(k)$ and apply (3.5) twice to obtain

$$\alpha_{hgh^{-1}}(k') = \alpha_h(\beta_g(\beta_{h^{-1}}(k')))\,\alpha_g(\beta_{h^{-1}}(k'))\,\alpha_{h^{-1}}(k') = \alpha_h(k)\,\alpha_g(k)\,\alpha_{h^{-1}}(k') = \alpha_g(k),$$

where the final equality follows from part (a). □

Our goal is to exploit the symmetry group G to reduce the number of independent variables of elements in X^{sym}. Before we move on to the general argument, we make some initial observations. Ultimately we shall restrict to those $c \in X^{\mathrm{sym}}$ which are also invariant under H, hence real-valued. It follows from $\gamma_{S_\tau} c = c$ that $c_k = 0$ whenever $k_1+k_2+k_3$ is odd. The following remark shows that this conclusion can also be reached using invariance under the group G only (i.e. without resorting to H).

Remark 3.6. *As warmup for what is to follow, we first consider*

$$G' \stackrel{\mathrm{def}}{=} \{g \in G \,:\, \beta_g = e\}. \tag{3.6}$$

The elements of G' act, by definition, trivially on the Fourier indices*, and they thus form a subgroup of G. In our case $G' = \{e, \gamma_{S_\pi}\}$, which is generated by the shift S_π in space. We note that G' is a normal subgroup of G, since the group homomorphism $\phi : g \to \beta_g$ has G' as its kernel. The quotient group G/G' is (isomorphic to) the point group O_h, the symmetry group of the cube.*

It follows from (3.5) *that $\alpha_g(k)$ is a group action of G' for each $k \in \mathbb{Z}^3$, since G' fixes k by definition* (3.6)*. For $c \in X$ to be invariant under the subgroup G', we must have that $\alpha_g(k)c_k = c_k$ for all $g \in G'$ and all $k \in \mathbb{Z}^3$, hence for each $k \in \mathbb{Z}^3$ we must have either $c_k = 0$ or $\alpha_g(k) = 1$ for all $g \in G'$. Since $\alpha_{\gamma_{S_\pi}}(k) = (-1)^{k_1+k_2+k_3}$ it follows that for any $c \in X^{\mathrm{sym}}$ it holds that $c_k = 0$ for $k \in \mathcal{Z}_{\mathrm{odd}}$, where*

$$\mathcal{Z}_{\mathrm{odd}} \stackrel{\mathrm{def}}{=} \{k \in \mathbb{Z}^3 : k_1 + k_2 + k_3 \text{ is odd}\}.$$

This illustrates how we can take advantages of the subgroup G', which acts trivially on all Fourier indices k, to reduce the number of variables by a factor 2 a priori. *To obtain further reductions of the number of independent variables using the full group G, we generalize these arguments below by considering each $k \in \mathbb{Z}^3$ separately.*

To simplify the presentation in what follows we use the notation

$$g.k \stackrel{\text{def}}{=} \beta_g(k) \qquad \text{for } g \in G.$$

For any $k \in \mathbb{Z}^3$ we define the stabilizer

$$G_k \stackrel{\text{def}}{=} \{g \in G \,:\, g.k = k\}.$$

and the orbit

$$G.k \stackrel{\text{def}}{=} \{g.k \,:\, g \in G\}.$$

Remark 3.7 (Orbit-stabilizer)**.** *The orbit-stabilizer theorem implies that $|G_{k'}| = |G_k|$ for all $k' \in G.k$, where $|\cdot|$ denotes the cardinality. Indeed, stabilizers of different elements in an orbit are related by conjugacy, and $|G| = |G_k| \cdot |G.k|$. More generally, when Q is a function from $\mathbb{Z}^3$ (or a relevant G-invariant subset thereof) to some linear space, then we have*

$$\sum_{g \in G} Q(g.k) = |G_k| \sum_{k' \in G.k} Q(k') \qquad \textit{for any } k \in \mathbb{Z}^3. \tag{3.7}$$

Lemma 3.8. *Let $k \in \mathbb{Z}^3$ be arbitrary. We have the following dichotomy:*
(a) *either $\alpha_g(k) = 1$ for all $g \in G_k$;*
(b) *or $\sum_{g \in G_k} \alpha_g(k) = 0$.*

Proof. Fix $k \in \mathbb{Z}^3$. We see from (3.5) that $\alpha_{g_1 g_2}(k) = \alpha_{g_1}(k)\alpha_{g_2}(k)$ for all $g_1, g_2 \in G_k$. Hence we can interpret $\alpha_g(k)$ as a group action of the stabilizer subgroup G_k, acting by multiplication on the unit circle $S^1 = \{z \in \mathbb{C} : |z| = 1\}$. We consider the stabilizer of $1 \in S^1$:

$$H_1 \stackrel{\text{def}}{=} \{g \in G_k : \alpha_g(k) = 1\},$$

and its orbit

$$O_1 \stackrel{\text{def}}{=} \{\alpha_g(k) : g \in G_k\}.$$

By the orbit-stabilizer theorem (we use Remark 3.7, but now for the group G_k-action $\alpha_g(k)$)

$$\sum_{g \in G_k} \alpha_g(k) = |H_1| \sum_{z \in O_1} z. \tag{3.8}$$

The set $O_1 \subset S^1$ is invariant under multiplication and division. In particular, if $|O_1| = N \in \mathbb{N}$, then $O_1 = \{e^{2\pi i n/N} : n = 0, 1, \ldots, N-1\}$. If $N = 1$ then we have $H_1 = G_k$ and alternative (a) follows, whereas if $N > 1$ then we see that $\sum_{z \in O_1} z = \sum_{n=0}^{N-1} e^{2\pi i n/N} = 0$, hence we conclude from (3.8) that alternative (b) holds. □

Remark 3.9. *The arguments in Lemma 3.8 are slightly more general than is strictly needed for the particular symmetry group under consideration in this paper. Namely, based on Remarks 3.3 and 3.6 we could have restricted to real-valued Fourier coefficients c_k while also* a priori *restricting the indices k to the ones where $k_1 + k_2 + k_3$ is even. It that case $\alpha_g(k)$ simplifies to an action on $\mathbb{R}$ consisting of multiplying by either $+1$ or -1, as is easily checked from the generators* (3.6)*. We present the more general argument here since it also applies to other symmetry groups (e.g. see [26, 23]).*

The indices for which alternative (b) in Lemma 3.8 applies are denoted by

$$\mathcal{Z}_{\text{triv}} \stackrel{\text{def}}{=} \Big\{k \in \mathbb{Z}^3 \,:\, \sum_{g \in G_k} \alpha_g(k) = 0\Big\}.$$

It follows from the next lemma, which is a slight generalization of Lemma 3.8, that the set $\mathcal{Z}_{\text{triv}}$ is invariant under G.

Lemma 3.10. *Let $k \in \mathbb{Z}^3$ be arbitrary. We have the following dichotomy:*
(a) *either $\alpha_g(k') = 1$ for all $g \in G_{k'}$ and all $k' \in G.k$;*
(b) *or $\sum_{g \in G_{k'}} \alpha_g(k') = 0$ for all $k' \in G.k$.*

Proof. Let $k \in \mathbb{Z}^3$ and $k' \in G.k$. Let $\widetilde{g} \in G$ be such that $\widetilde{g}.k = k'$. Then a conjugacy between G_k and $G_{k'}$ is given by $g \to \widetilde{g}g\widetilde{g}^{-1}$. It follows from Lemma 3.5(c) that

$$\sum_{g \in G_{k'}} \alpha_g(k') = \sum_{g \in G_k} \alpha_{\widetilde{g}g\widetilde{g}^{-1}}(k') = \sum_{g \in G_k} \alpha_g(k).$$

The assertion now follows from Lemma 3.8. □

When considering $c \in X^{\mathrm{sym}}$, the indices k in $\mathcal{Z}_{\mathrm{triv}}$ are the ones for which c_k necessarily vanishes.

Lemma 3.11. *Let $c \in X^{\mathrm{sym}}$. Then $c_k = 0$ for all $k \in \mathcal{Z}_{\mathrm{triv}}$.*

Proof. Fix $k \in \mathbb{Z}^3$. For any $c \in X^{\mathrm{sym}}$ we have in particular $[\gamma_g c]_k = c_k$ for all $g \in G_k$. By summing over $g \in G_k$ and using that $g.k = k$ for $g \in G_k$, we obtain

$$|G_k|\, c_k = \sum_{g \in G_k} c_k = \sum_{g \in G_k} (\gamma_g c)_k = \sum_{g \in G_k} \alpha_g(k) c_k = c_k \sum_{g \in G_k} \alpha_g(k).$$

If $k \in \mathcal{Z}_{\mathrm{triv}}$ then the right hand side vanishes, hence $c_k = 0$. □

It follows from the dichotomy in Lemma 3.8 that $k \in \mathcal{Z}_{\mathrm{triv}}$ if there is a $g \in G_k$ such that $\alpha_g(k) \neq 1$, hence this construction generalizes the argument in Remark 3.6.

Lemma 3.11 implies that

$$X^{\mathrm{sym}} \subset \{c \in X \,:\, c_k = 0 \text{ for all } k \in \mathcal{Z}_{\mathrm{triv}}\}.$$

In other words, we may restrict attention to the Fourier coefficients corresponding to indices in the complement

$$\mathcal{Z}_{\mathrm{sym}} \stackrel{\mathrm{def}}{=} \mathbb{Z}^3 \setminus \mathcal{Z}_{\mathrm{triv}}.$$

Remark 3.12. *On S^1 we have $z^{-1} = z^*$, and $(z_1 + z_2)^{-1} = z_1^{-1} + z_2^{-1}$. In particular, Lemma 3.8 implies that*

$$\sum_{g \in G_k} \alpha_g(k) = \sum_{g \in G_k} \alpha_g^{-1}(k) = \begin{cases} 0 & \text{for } k \in \mathcal{Z}_{\mathrm{triv}}, \\ |G_k| & \text{for } k \in \mathcal{Z}_{\mathrm{sym}}. \end{cases}$$

The sum with the inverses is computed in the code, both to identify the set $\mathcal{Z}_{\mathrm{triv}}$ and to determine $|G_k|$ for $k \in \mathcal{Z}_{\mathrm{sym}}$.

For $c \in X^{\mathrm{sym}}$ the coefficients c_k with $k \in \mathcal{Z}_{\mathrm{sym}}$ are not all independent. To take advantage of this, we choose a fundamental domain of G in $\mathbb{Z}^3$:

$$\mathcal{Z}_{\mathrm{dom}} = \{k \in \mathbb{Z}^3 \,:\, 0 \leq k_3 \leq k_2 \leq k_1\}, \tag{3.9}$$

i.e., $\mathcal{Z}_{\mathrm{dom}}$ contains precisely one element of each group orbit. In fact, the arguments below are independent of which fundamental domain one chooses. The above choice is the one used in the code. We now define the set of *symmetry reduced indices* as

$$\mathcal{Z} \stackrel{\mathrm{def}}{=} \mathcal{Z}_{\mathrm{dom}} \cap \mathcal{Z}_{\mathrm{sym}},$$

and the space of *symmetry reduced variables* as

$$\mathbf{X} \stackrel{\mathrm{def}}{=} \Big\{(b_k)_{k \in \mathcal{Z}} \,:\, b_k \in \mathbb{R} \,:\, \sum_{k \in \mathcal{Z}} |b_k| < \infty\Big\}.$$

The choice of taking real-valued variables b_k stems from Remark 3.3. In slight abuse of notation we will also interpret e_k with $k \in \mathcal{Z}$ as elements of $\mathbf{X}$. We note that the action γ_g on these basis vectors is

$$(\gamma_g \mathrm{e}_k)_{k'} = \alpha_g(k')\delta_{k\beta_g(k')} = \alpha_g(k')\delta_{\beta_{g^{-1}}(k)k'} = \alpha_g(k')(\mathrm{e}_{g^{-1}.k})_{k'}\,,$$

hence

$$\gamma_g \mathrm{e}_k = \alpha_g(g^{-1}.k)\mathrm{e}_{g^{-1}.k}\,. \tag{3.10}$$

Before we specify the dependency of the coefficients $\{c_k\}_{k\in\mathcal{Z}_{\mathrm{sym}}}$ on the symmetry reduced variables $\{c_k\}_{k\in\mathcal{Z}}$ for $c \in X^{\mathrm{sym}}$, we derive some additional properties of $\alpha_g(k)$ for $k \in \mathcal{Z}_{\mathrm{sym}}$.

Lemma 3.13. *Let $g_1, g_2 \in G$ and $k \in \mathcal{Z}_{\mathrm{sym}}$. If $g_1.k = g_2.k$, then $\alpha_{g_1}(k) = \alpha_{g_2}(k)$.*

Proof. Since $g_2^{-1}g_1.k = k$ and $k \in \mathcal{Z}_{\mathrm{sym}}$ we have $\alpha_{g_2^{-1}g_1}(k) = 1$ by Lemma 3.8(a). An application of Lemma 3.5(b) concludes the proof. □

Definition 3.14. *Let k be any element of $\mathcal{Z}_{\mathrm{sym}}$ and k' any element in its orbit $G.k$. We can choose a $\widetilde{g} = \widetilde{g}(k,k') \in G$ such that $\widetilde{g}.k = k'$. For such k and k' we define*

$$\widetilde{\alpha}(k,k') \stackrel{\mathrm{def}}{=} \alpha^{-1}_{\widetilde{g}(k,k')}(k) \qquad \text{for } k \in \mathcal{Z}_{\mathrm{sym}} \text{ and } k' \in G.k.$$

This is independent of the choice of $\widetilde{g}$ by Lemma 3.13, and clearly

$$\alpha_g^{-1}(k) = \widetilde{\alpha}(k, g.k) \qquad \text{for all } k \in \mathcal{Z}_{\mathrm{sym}} \text{ and } g \in G. \tag{3.11}$$

We are now ready to symmetrize elements of $\mathbf{X}$. To convert from an element $b \in \mathbf{X}$ to an element $c \in X^{\mathrm{sym}}$ we apply the symmetrization

$$\sigma(b) \stackrel{\mathrm{def}}{=} \sum_{k\in\mathcal{Z}} b_k \sum_{k'\in G.k} \widetilde{\alpha}(k,k')\mathrm{e}_{k'}. \tag{3.12}$$

Lemma 3.15. *Let $b \in \mathbf{X}$. Then $\sigma(b) \in X^{\mathrm{sym}}$ and $\sigma(b)_k = b_k$ for $k \in \mathcal{Z}$. Furthermore, $\sigma(b)_k \in \mathbb{R}$ for all $k \in \mathbb{Z}^3$.*

Proof. For $b \in \mathbf{X}$ we define

$$\tilde{b} \stackrel{\mathrm{def}}{=} \sum_{k\in\mathcal{Z}} \frac{b_k}{|G_k|}\mathrm{e}_k.$$

To show that $\sigma(b) \in X^{\mathrm{sym}}$ it suffices to prove that it is the group average of $\tilde{b}$:

$$\sigma(b) = \sum_{g\in G} \gamma_g \tilde{b}. \tag{3.13}$$

Namely, by (3.10) and Lemma 3.5(a),

$$\begin{aligned}
\sum_{g\in G} \gamma_g \tilde{b} &= \sum_{k\in\mathcal{Z}} b_k \frac{1}{|G_k|} \sum_{g\in G} \gamma_g \mathrm{e}_k \\
&= \sum_{k\in\mathcal{Z}} b_k \frac{1}{|G_k|} \sum_{g\in G} \alpha_g(g^{-1}.k)\mathrm{e}_{g^{-1}.k} \\
&= \sum_{k\in\mathcal{Z}} b_k \frac{1}{|G_k|} \sum_{g\in G} \alpha_{g^{-1}}(g.k)\mathrm{e}_{g.k} \\
&= \sum_{k\in\mathcal{Z}} b_k \frac{1}{|G_k|} \sum_{g\in G} \alpha_g^{-1}(k)\mathrm{e}_{g.k} \\
&= \sum_{k\in\mathcal{Z}} b_k \frac{1}{|G_k|} \sum_{g\in G} \widetilde{\alpha}(k,g.k)\mathrm{e}_{g.k} \\
&= \sum_{k\in\mathcal{Z}} b_k \sum_{k'\in G.k} \widetilde{\alpha}(k,k')\mathrm{e}_{k'},
\end{aligned}$$

where in the penultimate equality we have used (3.11), while the final equality follows from (3.7) with $Q(k') = \widetilde{\alpha}(k,k')\mathrm{e}_{k'}$ (for fixed $k \in \mathcal{Z}$).

The assertion that $\sigma(b)_k = b_k$ for $k \in \mathcal{Z}$ follows directly from (3.12) and $\widetilde{\alpha}(k,k) = 1$. Finally, it follows from Remark 3.9 that $\widetilde{\alpha}(k,k') \in \{-1,1\}$. Since $b_k \in \mathbb{R}$ for all $k \in \mathcal{Z}$, Equation (3.12) implies that $\sigma(b)_k \in \mathbb{R}$ for all $k \in \mathbb{Z}^3$. □

The following converse of Lemma 3.15 holds. Note that we do not restrict to real-valued c here.

Lemma 3.16. *Let $c \in X^{\mathrm{sym}}$. Define $b = \sum_{k\in\mathcal{Z}} c_k \mathrm{e}_k$. Then $\sigma(b) = c$.*

Proof. Let $\tilde{c} = c - \sigma(b)$. Then $\tilde{c} \in X^{\mathrm{sym}}$ and $\tilde{c}_{k'} = 0$ for all $k' \in \mathcal{Z}$ by Lemma 3.15. Consider any fixed $k' \in \mathcal{Z}_{\mathrm{sym}}$, then there exists a $k \in \mathcal{Z} \cap G.k'$. Let $\widetilde{g} \in G$ be such that $\widetilde{g}.k = k'$. Since $\tilde{c} \in X^{\mathrm{sym}}$ we have

$$\alpha_{\widetilde{g}}(k)\tilde{c}_{k'} = (\gamma_{\widetilde{g}}\tilde{c})_k = \tilde{c}_k = 0.$$

Since $\alpha_{\widetilde{g}}(k) \in S^1$ this implies that $\tilde{c}_{k'} = 0$, and since $k' \in \mathcal{Z}_{\mathrm{sym}}$ was arbitrary, we conclude that $\tilde{c}_{k'} = 0$ for all $k' \in \mathcal{Z}_{\mathrm{sym}}$. Finally, it then follows from Lemma 3.11 that

$$\tilde{c} = \sum_{k\in\mathbb{Z}^3} \tilde{c}_k \mathrm{e}_k = \sum_{k\in\mathcal{Z}_{\mathrm{triv}}} \tilde{c}_k \mathrm{e}_k = 0 + \sum_{k\in\mathcal{Z}_{\mathrm{sym}}} \tilde{c}_k \mathrm{e}_k = 0.$$

Hence $c = \sigma(b)$. □

On $\mathbf{X}$ we use the 1-norm weighted by the multiplicity of each coefficient in the symmetry class:

$$\|b\|_{\mathrm{s}} \stackrel{\mathrm{def}}{=} \sum_{k\in\mathcal{Z}} |G.k|\,|b_k|\,.$$

In particular, $\|\mathrm{e}_k\|_{\mathrm{s}} = |G.k|$ for $k \in \mathcal{Z}$. We recall that $|G.k| = |G|/|G_k|$ by Remark 3.7. This observation is combined with Remark 3.12 to determine the weights $|G.k|$ in the code. The next lemma shows that the norm $\|b\|_{\mathrm{s}}$ is compatible with the symmetrization.

Lemma 3.17. *For all $b \in \mathbf{X}$ we have $\|b\|_{\mathrm{s}} = \|\sigma(b)\|$.*

Proof. From the definition (3.12) we obtain

$$\|\sigma(b)\| = \sum_{k\in\mathcal{Z}} \sum_{k'\in G.k} |b_k\,\widetilde{\alpha}(k,k')| = \sum_{k\in\mathcal{Z}} |b_k| \sum_{k'\in G.k} |\widetilde{\alpha}(k,k')| = \sum_{k\in\mathcal{Z}} |b_k|\,|G.k| = \|b\|_{\mathrm{s}}\,,$$

since $\widetilde{\alpha} \in S^1$. □

3.3 The functional analytic setup in symmetry reduced variables

We are now able to reconsider the formulation outlined in Subsections 2.2-2.4 in the symmetry reduced variables.

Since the average is fixed ($c_0 = m$), it is convenient to introduce

$$\mathcal{Z}_0 \stackrel{\mathrm{def}}{=} \mathcal{Z} \setminus \{0\},$$

and

$$\mathbf{X}_0 \stackrel{\mathrm{def}}{=} \{b \in \mathbf{X} \,:\, b_0 = 0\}.$$

Any $b \in \mathbf{X}_0$ can be expressed as $b = \sum_{k\in\mathcal{Z}_0} b_k \mathrm{e}_k$. Observing that σ maps $\mathbf{X}_0$ to X_0, we define the map F with domain $\mathbf{X}_0$ by

$$F_k(b) \stackrel{\mathrm{def}}{=} f_k(\sigma(b)), \tag{3.14}$$

where we recall that $f_k(c) = h_k(m\mathrm{e}_0 + c)$, with h defined in (2.1) and (2.2). It is trivial that

$$f_0(c) = 0 \qquad \text{for any } c \in X_0, \tag{3.15}$$

hence we may interpret f as a map from X_0 to X_0. We note that X_0 is invariant under the action γ of G. Since the PDE (1.1) is equivariant under the symmetries (1.3), it follows that the map $f : X_0 \to X_0$, which is the Fourier transform of (1.1), is equivariant, as formalized in the next lemma.

Lemma 3.18. *Let $g \in G$. We have*

$$h(\gamma_g c) = \gamma_g h(c) \qquad \text{for all } c \in X, \tag{3.16}$$
$$f(\gamma_g c) = \gamma_g f(c) \qquad \text{for all } c \in X_0. \tag{3.17}$$

Proof. Since $\gamma_g \mathrm{e}_0 = \mathrm{e}_0$, it follows from (2.2) that $[h(\gamma_g c)]_0 = [\gamma_g h(c)]_0$. Since $\mathbf{k}$ is invariant under the action β_g, the linear term in (2.1) is equivariant. Equivariance of the nonlinear term follows from Lemma 3.4. This proves (3.16). Finally, by using again that $\gamma_g \mathrm{e}_0 = \mathrm{e}_0$ we infer that

$$f(\gamma_g c) = h(m\mathrm{e}_0 + \gamma_g c) = h(\gamma_g(m\mathrm{e}_0 + c)) = \gamma_g h(m\mathrm{e}_0 + c) = \gamma_g f(c),$$

which establishes (3.17). □

Next, we establish the fact that we may use the symmetry reduced variables $\mathbf{X}_0$ to obtain symmetric solutions.

Lemma 3.19. *Let $b \in \mathbf{X}_0$. If $F_k(b) = 0$ for $k \in \mathcal{Z}_0$, then $F_k(b) = 0$ for all $k \in \mathbb{Z}^3$, and*

$$u(x) = m + \sum_{k \in \mathbb{Z}^3_0} \sigma(b)_k \, e^{ik\cdot x/\ell} \tag{3.18}$$

is a real-valued solution of (1.1) which is $\mathcal{G}$-symmetric in the sense of Definition 1.1.

Proof. Since $\sigma(b) \in X^{\mathrm{sym}}$ by Lemma 3.15, it follows from (3.17) that $\gamma_g f(\sigma(b)) = f(\gamma_g \sigma(b)) = f(\sigma(b))$, hence $f(\sigma(b)) \in X^{\mathrm{sym}}$. By Lemma 3.16 this implies that

$$f(\sigma(b)) = \sigma(\tilde{f}), \tag{3.19}$$

where

$$\tilde{f} \stackrel{\mathrm{def}}{=} \sum_{k \in \mathcal{Z}} f_k(\sigma(b))\mathrm{e}_k = f_0(\sigma(b)) + \sum_{k \in \mathcal{Z}_0} F_k(b)\mathrm{e}_k.$$

By assumption, $F_k(b) = 0$ for all $k \in \mathcal{Z}_0$, and since $f_0(\sigma(b))$ vanishes by (3.15) as well, we see that $\tilde{f} = 0$. We conclude from (3.19) that $F_k(b) = f_k(\sigma(b)) = 0$ for all $k \in \mathbb{Z}^3$.

Finally, let $c = m\mathrm{e}_0 + \sigma(b)$, then Lemma 3.15 shows that $c \in X^{\mathrm{sym}}$ and $c_k \in \mathbb{R}$ for all $k \in \mathbb{Z}^3$. Hence it follows from Lemma 3.2 that $u(x) = \sum_{k \in \mathbb{Z}^3} c_k e^{ik\cdot x/\ell}$ is a real-valued $\mathcal{G}$-symmetric function. Moreover, $u(x)$ solves (1.1) because $h(c) = 0$, which is the Fourier equivalent of (1.1). □

3.4 The fixed point operator

To solve the zero finding problem $F = 0$ on $\mathbf{X}_0$, we set up a fixed point operator as in Section 2. The role of X_0 is taken over by $\mathbf{X}_0$, and the norm $\|\cdot\|$ is replaced by the weighted norm $\|\cdot\|_{\mathrm{s}}$, which is symmetry compatible in the sense of Lemma 3.17. The size of the Galerkin projection is

$$N = N^{\mathrm{sym}}(K) \stackrel{\mathrm{def}}{=} |\{k \in \mathcal{Z}^3 \,:\, 0 < \mathbf{k} \le K\}|,$$

which is substantially smaller than $N(K)$ as defined in (2.10), since we restrict to symmetry reduced variables. Indeed, the number of independent variables is reduced by roughly a factor $|G| = 96$, which splits into a factor roughly 48 due to restricting to a fundamental domain $\mathcal{Z}_{\mathrm{dom}}$ (see (3.9)), and a factor roughly 2 thanks to restricting k to $\mathcal{Z}_{\mathrm{sym}} = \mathbb{Z}^3 \setminus \mathcal{Z}_{\mathrm{triv}}$ with $\mathcal{Z}_{\mathrm{odd}} \subset \mathcal{Z}_{\mathrm{triv}}$, see Remark 3.6. The construction of the operator $T : \mathbf{X}_0 \to \mathbf{X}_0$ is essentially unchanged compared to Section 2. While the construction of the approximate inverse in the symmetrized setting is essentially the same as in Section 2, for clarity we will denote it by A^{s} and write

$$T(b) = b - A^{\mathrm{s}} F(b).$$

Theorem 2.1 remains valid, and by Lemma 3.19 this produces a symmetric solution of (1.1). In sections 3.5 and 3.6 we discuss the changes that the symmetric setting causes in the explicit expression for the bounds Y and $Z(r)$, respectively.

3.5 The bound Y

There are essentially no changes compared to Section 2.3 in the computation of the bound on the residue, except that we need to take into account the symmetry respecting norm:

$$Y = \uparrow \sum_{k \in \mathcal{Z}_0, \mathbf{k} \le 3K} |G.k| \left| A^{\mathrm{s}} F_k(\bar{b}) \right|. \tag{3.20}$$

3.6 The bound Z

We will comment only on the changes compared to Section 2.4 due to the symmetric setting. The most important change is in the formula (2.21) for the derivative. It follows from the definition of F in (3.14) and the formula (3.12) for the symmetrization σ that

$$DF_k(b)\mathrm{e}_{k'} = \delta_{kk'}\lambda_k + 3\ell^{-2}\mathbf{k}^2 \sum_{k'' \in G.k'} \widetilde{\alpha}(k', k'') \langle (\sigma(m\mathrm{e}_0 + b))^2 \rangle_{k-k''}, \qquad \text{for } k, k' \in \mathcal{Z}_0.$$

Taking into account this new expression for the Jacobian, the bound Q_1 is essentially unchanged, except that we need to use the weighted norm. We obtain

$$Q_1 = \uparrow \max_{k' \in \mathcal{Z}_0, \mathbf{k}' \le K} \frac{1}{|G.k'|} \sum_{k \in \mathcal{Z}_0, \mathbf{k} \le K} |G.k| \left| (I_N - A^{\mathrm{s}}_N J_N)_{kk'} \right|. \tag{3.21}$$

For the bound Q_2 we observe that, with $k, k' \in \mathcal{Z}$,

$$([DF(\bar{b}) - J]\mathrm{e}_{k'})_k = \begin{cases} 0 & \text{for } \mathbf{k}', \mathbf{k} \le K, \\ 3\ell^{-2}\mathbf{k}^2 \sum_{k'' \in G.k'} \widetilde{\alpha}(k', k'') \langle (\sigma(m\mathrm{e}_0 + \bar{b}))^2 \rangle_{k-k''} & \text{otherwise.} \end{cases} \tag{3.22}$$

Note that $([DF(\bar{b}) - J]\mathrm{e}_{k'})_k = 0$ for $\mathbf{k} \le K$ and $\mathbf{k}' > 3K$. We thus use the same splitting in the tail $\mathbf{k}' > 3K$ and the finite part $\mathbf{k}' \le 3K$ as in Section 2. Taking the symmetry reduced variables into account, we obtain

$$\widetilde{Q}_2 = \uparrow \max_{k' \in \mathcal{Z}_0, \mathbf{k}' \le 3K} \frac{1}{|G.k'|} \left\| A^{\mathrm{s}} [DF(\bar{b}) - J]\mathrm{e}_{k'} \right\|_{\mathrm{s}},$$

which is evaluated using (3.22). We obtain

$$Q_2 = \max\{\widetilde{Q}_2, \uparrow 3C_K \| \langle (\sigma(m\mathrm{e}_0 + \bar{b}))^2 \rangle \|\}, \tag{3.23}$$

with C_K defined in (2.26).

Next, for Q_3 we again follow the arguments of Section 2. We define, for $q \in \mathbf{X}$, $k \in \mathcal{Z}_0$

$$(\widetilde{P}q)_k \stackrel{\mathrm{def}}{=} 6\ell^{-2}\mathbf{k}^2 \langle \sigma(m\mathrm{e}_0 + \bar{b}) \sigma(q) \rangle_k,$$

and we estimate the norm of $A^{\mathrm{s}}\widetilde{P}$ by (using Lemma 3.17)

$$Q_{3,1} = \max\{\widetilde{Q}_{3,1}, \uparrow 6C_K \| m\mathrm{e}_0 + \bar{b} \|_{\mathrm{s}}\}, \tag{3.24}$$

where

$$\widetilde{Q}_{3,1} = \uparrow \max_{k' \in \mathcal{Z}, \mathbf{k}' \le 2K} \frac{1}{|G.k'|} \| A^{\mathrm{s}} \widehat{P}(k') \|_{\mathrm{s}},$$

with

$$\widehat{P}_k(k') = 6\ell^{-2}\mathbf{k}^2 \sum_{k'' \in G.k'} \widetilde{\alpha}(k', k'') (\sigma(m\mathrm{e}_0 + \bar{b}))_{k-k''}, \qquad \text{for } k' \in \mathcal{Z}.$$

Finally, by using analogous arguments the quadratic term in r is estimated by

$$Q_{3,2} = \max\{\widetilde{Q}_{3,2}, \uparrow 3C_K\}, \tag{3.25}$$

where

$$\widetilde{Q}_{3,2} = \uparrow \max_{k' \in \mathcal{Z}, 0 < \mathbf{k}' \le K} \frac{1}{|G.k'|} \| A^{\mathrm{s}} \widehat{R}(k') \|_{\mathrm{s}},$$

with

$$\widehat{R}_k(k') = 3\ell^{-2}\mathbf{k}^2 \delta_{kk'}.$$

3.7 Extensions

Whenever we mentioned specific generators, we have focussed on space group 230. The other example used in this paper is space group 229, which is generated by

$$\begin{aligned} S_\sigma x &= (x_2, x_3, x_1), \\ S_\phi x &\stackrel{\text{def}}{=} (x_2, x_1, x_3), \\ S_\psi x &\stackrel{\text{def}}{=} (-x_1, x_2, x_3), \\ S_\tau^2 x &= \left(x_1 + \tfrac{L}{2}, x_2 + \tfrac{L}{2}, x_3 + \tfrac{L}{2}\right). \end{aligned}$$

The conversion to the group action on Fourier space via Remark 3.1 is straightforward. We note that S_π, see (1.4), is an element of the group, hence we may restrict attention to real Fourier coefficients as for the space group 230. Furthermore, the same fundamental domain $\mathcal{Z}_{\rm dom}$ can be chosen as for space group 230.

Although we focus in this paper on the two space groups 229 and 230 only, the symmetry preserving formulation in this section can be applied much more generally (e.g. see [26, 23]). If the symmetries are such that we may not restrict to real Fourier coefficients (i.e. in case $(x_1, x_2, x_3) \to (-x_1, -x_2, -x_3)$ is not a symmetry), then there are two ways to proceed to include the symmetry coming from the real-valuedness of $u(x)$. The first is to simply not include this symmetry in G (i.e. ignoring $c^*_{-k} = c_k$). A disadvantage of this approach is that the number of symmetry reduced variables is sub-optimal. An advantage is that one one can still work over complex numbers. The final symmetry of the solution ($c^*_{-k} = c_k$, i.e., the solution u is real) can then be recovered via the equivariance arguments in Remark 2.3.

The second possibility is to include the symmetry with action $(k_1, k_2, k_3) \to (-k_1, -k_2, -k_3)$ on $\mathbb{Z}^3$ in G, with corresponding action $c_k \to c^*_{-k}$ on the Fourier coefficients. This leads to an optimal reduction in the number of symmetry reduced variables (and thus reduced memory usage). However, one needs to separate all Fourier coefficients into real and imaginary parts and work with those real variables. This is a little more cumbersome than working with complex variables. We did not need to pursue either of these approaches for the symmetry groups under consideration.

3.8 Symmetry in the code

The main symmetry operation in the code is averaging over de group action, which is performed in `symmetrize.m`. In the notation of this paper, it is a function $\mathtt{S}$ with as input an element of X_N, see (2.11), and as output an element of $X_N \cap X^{\rm sym}$. To be precise,

$$\begin{aligned} \mathtt{S}(c) &\stackrel{\text{def}}{=} \sum_{g \in G} \gamma_g c \\ &= \sum_{g \in G} \sum_{\mathbf{k} \le K} c_k \, \alpha_g^{-1}(k) \, \mathrm{e}_{g.k}. \end{aligned} \tag{3.26}$$

We note that $\mathtt{S}$ is closely related to the symmetrization σ defined in (3.12), see also (3.13). In particular, interpreting $b = \sum_{k \in \mathcal{Z}, \mathbf{k} \le K} b_k \mathrm{e}_k \in \mathbf{X}$ as an element of X_N, we have

$$\sigma(b)_k = \frac{\mathtt{S}(b)_k}{|G_k|} \qquad \text{for all } k \in \mathbb{Z}^3.$$

The effectiveness of the code is based on the following property of $\mathtt{S}$. Let

$$1_{\rm dom} \stackrel{\text{def}}{=} \sum_{k \in \mathcal{Z}_{\rm dom}} \mathrm{e}_k$$

be the indicator function of the fundamental domain. Fix any $k' \in \mathbb{Z}^3$, and let $k = G.k' \cap \mathcal{Z}_{\rm dom}$. Then

$$\mathtt{S}(1_{\rm dom})_{k'} = \begin{cases} 0 & k' \in \mathcal{Z}_{\rm triv}, \\ \widetilde{\alpha}(k, k') \, |G_{k'}| & k' \in \mathcal{Z}_{\rm sym}. \end{cases}$$

Namely, let $\widetilde{g}$ be such that $\widetilde{g}.k = k'$. Then using (3.26), the orbit-stabilizer theorem, the multiplication property (3.5) of α (and α^{-1}), Lemma 3.8, Remark 3.12 and (3.11), we obtain

$$\begin{aligned}
\mathtt{S}(1_{\mathrm{dom}})_{k'} &= \sum_{g\in G, g.k=k'} \alpha_g^{-1}(k) \\
&= \sum_{g\in G_k} \alpha_{\widetilde{g}g}^{-1}(k) \\
&= \sum_{g\in G_k} \alpha_{\widetilde{g}}^{-1}(g.k)\, \alpha_g^{-1}(k) \\
&= \alpha_{\widetilde{g}}^{-1}(k) \cdot \begin{cases} 0 & k \in \mathcal{Z}_{\mathrm{triv}} \\ |G_k| & k \in \mathcal{Z}_{\mathrm{sym}} \end{cases} \\
&= \begin{cases} 0 & k' \in \mathcal{Z}_{\mathrm{triv}} \\ \widetilde{\alpha}(k,k')\,|G_{k'}| & k' \in \mathcal{Z}_{\mathrm{sym}}. \end{cases}
\end{aligned}$$

As a consequence $|\mathtt{S}(1_{\mathrm{dom}})_{k'}| = |G_{k'}|$ for all $k' \in \mathcal{Z}_{\mathrm{sym}}$. In particular, $\mathtt{S}(1_{\mathrm{dom}})_0$ equals the order of the symmetry group.

4 Results

4.1 Implementation

Given a numerically computed approximation $\bar{u}(x)$, expressed in terms of finitely many Fourier modes, of a solution to (1.1), in order to prove that a nearby (true) solution $\hat{u}(x)$ exists (c.f. Remark 2.2 and (2.19)), we proceed as follows:

1. Compute the finite Jacobian J_N numerically.
2. Numerically invert the finite Jacobian to find A_N^{s}.
3. Define the parameters m, γ and l and A_N^{s} as interval objects.
4. Evaluate the residual bound Y using (3.20).
5. Evaluate the terms Q_1, Q_2, $Q_{3,1}$ and $Q_{3,2}$ as defined in (3.21), (3.23), (3.24) and (3.25) respectively.
6. Form the radii polynomial $p(r) = Y + r(Q_1 + Q_2 + rQ_{3,1} + r^2 Q_{3,2}) - r$.
7. Seek the roots $r_-, r_+ > 0$ such that $p(r) < 0$ for $r_- < r < r_+$.

If the last step is succesful then we have proven the existence of a solution $\hat{u}(x)$, satisfying

$$\|\hat{u}(x) - \bar{u}(x)\|_\infty \leq r_-.$$

If not, we extend the numerical approximate solution to a larger value of K (more Fourier modes), iterate Newton's method until convergence and try again. This procedure does not lead to the smallest possible r_-, but rather focusses on obtaining the "cheapest" proof (small K). If our goal would be to minimize r_- we could simply increase K (at computational cost of course).

We enforce the symmetry of the solution as outlined in Section 3. This does not just ensure that the proven solution has the required symmetry. It also significantly reduces the computational cost. In particular, we compute on the Fourier coefficients $(b_k)_{k\in\mathcal{Z},\mathbf{k}\leq K}$ only. For space groups 230 this reduces the number of variables by roughly a factor 200, for example with $K = 37$, only 2221 modes are used out of 421875 possible. This also reduces the size of the matrices J_N and A_N^{s} by a factor $O(10^4)$. One crucial aspect of the effective algorithmic implementation of both the symmetry reduced indices and symmetry reduced variables is explained 3.8. The general algorithm is the

Double gyroids				
Label	m	γ	ℓ	K
(a)	0.02	2.1	1.75	9
(b)	0.04	3	1.5	19
(c)	0.05	4	1.3	27
(d)	0.06	5	1.2	37
(e)	0.1	2.1	1.75	9
(f)	0.25	3	1.5	19
(g)	0.3	4	1.3	27
(h)	0.35	5	1.2	37

bcc-packed spheres				
Label	m	γ	ℓ	K
(a)	0.02	2.1	1	4
(b)	0.04	3	0.8	11
(c)	0.05	4	0.75	13
(d)	0.06	5	0.7	19
(e)	0.1	2.1	1	4
(f)	0.25	3	0.8	9
(g)	0.3	4	0.75	13
(h)	0.35	5	0.7	17

Table 1: Parameter values for double gyroids and bcc-packed spheres. The labels refer to Figures 4.1 and 4.2.

same for all symmetry groups. With the basic structure in place, implementing each additional space group only requires a few additional lines of code (generating all the elements of the group action).

We used this method to prove the existence of both *double gyroids* from space group 230, see Figure 4.1, and *bcc-packed spheres* from space group 229, see Figure 4.2. Additionally, "exotic" symmetric stationary states were proven to exist, see Figure 4.3. The physical and computational parameters for these proofs can be found in Section 4.2.

All proofs were implemented in Matlab using the interval toolbox IntLab [18, 19]. The required estimates and bounds for the fixed point proofs are all verified with interval arithmetic to avoid any possible floating point errors. Verifiable data files, including all parameter values used in the computational proofs, and code are available at [27].

4.2 Computational Details

All computations were performed on an early 2016 MacBook taking between a few seconds and minutes to find small finite approximations. Running the proof requires more modes and takes between a few minutes and several hours, scaling like $O(K^6)$.

To find double gyroid and bcc-packed sphere solutions, we started with parameters values (m, γ) near the bifurcation point $(0, 2)$. There, to leading order, the Fourier coefficients can be computed by hand. We then continued in the parameters to obtain solutions for larger parameter vales.

The parameter values m, γ and ℓ for the proven double gyroids and proven bcc-packed spheres are collected in Table 1. The values of K used in the proofs are also given there. These values of K are near minimal for the proofs to work, but in some cases $K - 1$ may also have been sufficient. More modes are required as γ increases, as the solutions develop sharper transitions between $u > m$ and $u < m$ (in the limit $\gamma \to \infty$ solutions tend to profiles which are $u = \pm 1$ almost everywhere). Note that we need more modes to prove the double gyroid than for the spheres.

In addition to double gyroids and spheres, by starting Newton's method with random initial data we also encountered a number of more exotic profiles, showcasing the richness of the model and the complexity of the energy landscape. In Figure 4.3 we present some of the more interesting ones we found in space group 230. These profiles were all proven to exist with $m = 0.2$ and $\gamma = 3$, whilst the other parameters varied, see the caption of Figure 4.3. Of particular note are the mixture of cylinders and spheres and the deformed double gyroid. The latter has the same triple junctions as the double gyroid but the intersections occur at right angles. The interlocking cylinders may be related to the "woodpile" solution mentioned in [14].

5 Conclusions and future work

We have presented the first rigorous proof of existence of double gyroid solutions for the stationary Ohta-Kawasaki problem in three dimensions, as well as bcc-packed spheres and additional exotic

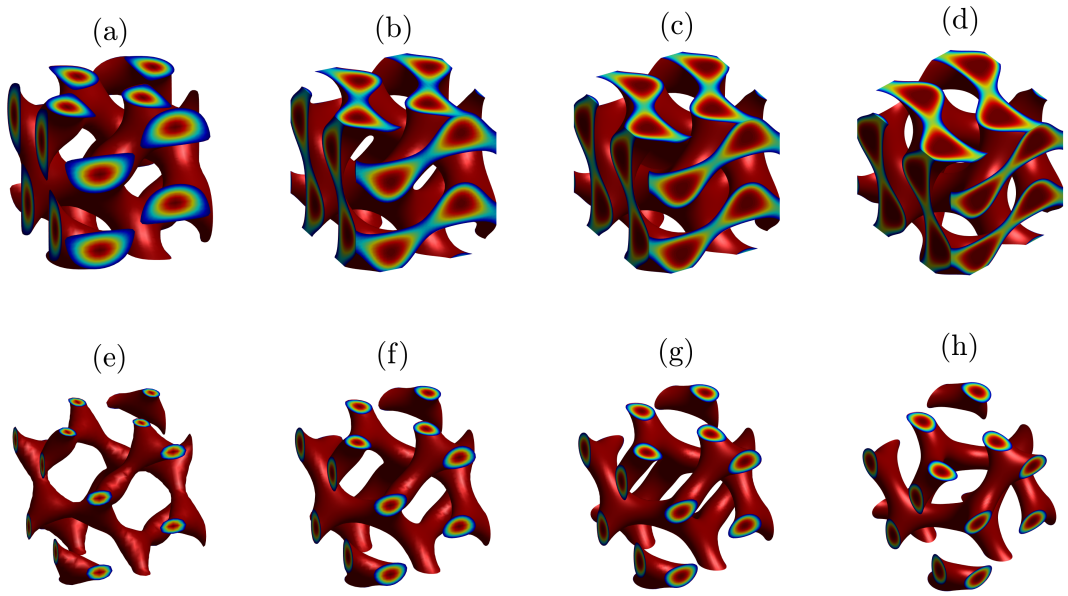

Figure 4.1: Double gyroids. The parameters m and γ both increase from left to right. In the bottom row the values of m are larger than in the top row, see Table 1 for parameter values. The level sets in the top row are plotted at $u(x, y, z) = -m$, while in the bottom to we selected the level set $u(x, y, z) = -2m$. These levels are chosen for display purposes only. Each image has been rotated to give a slightly different view.

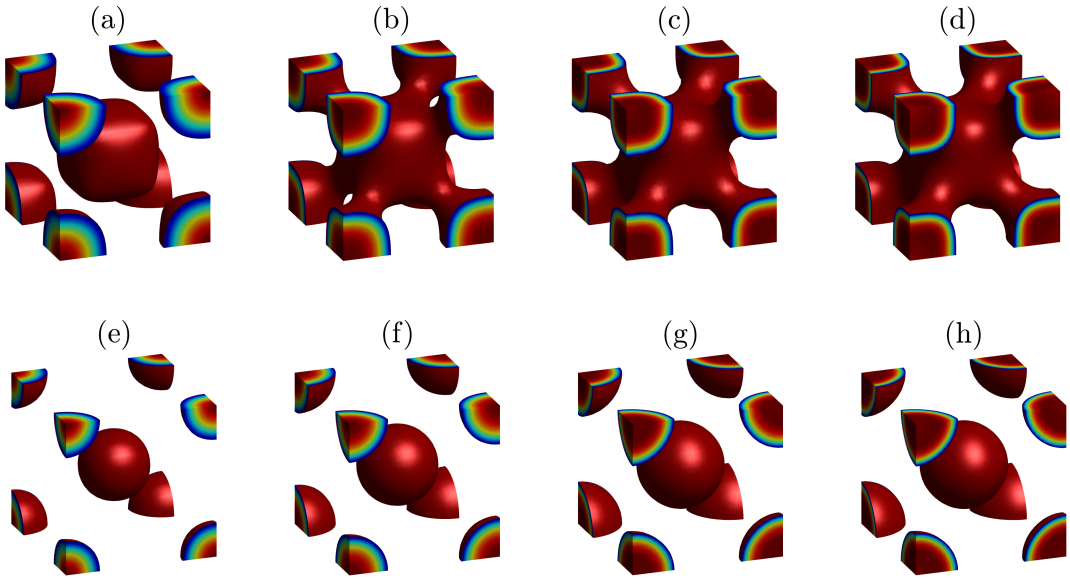

Figure 4.2: bcc-packed structures. The parameters m and γ both increase from left to right. In the bottom row the values of m are larger than in the top row, see Table 1 for parameter values. The level sets are all plotted at $u(x, y, z) = -m$ for clarity and consistency. We note that the upper row would show disconnected (spherical) structures for different level sets.

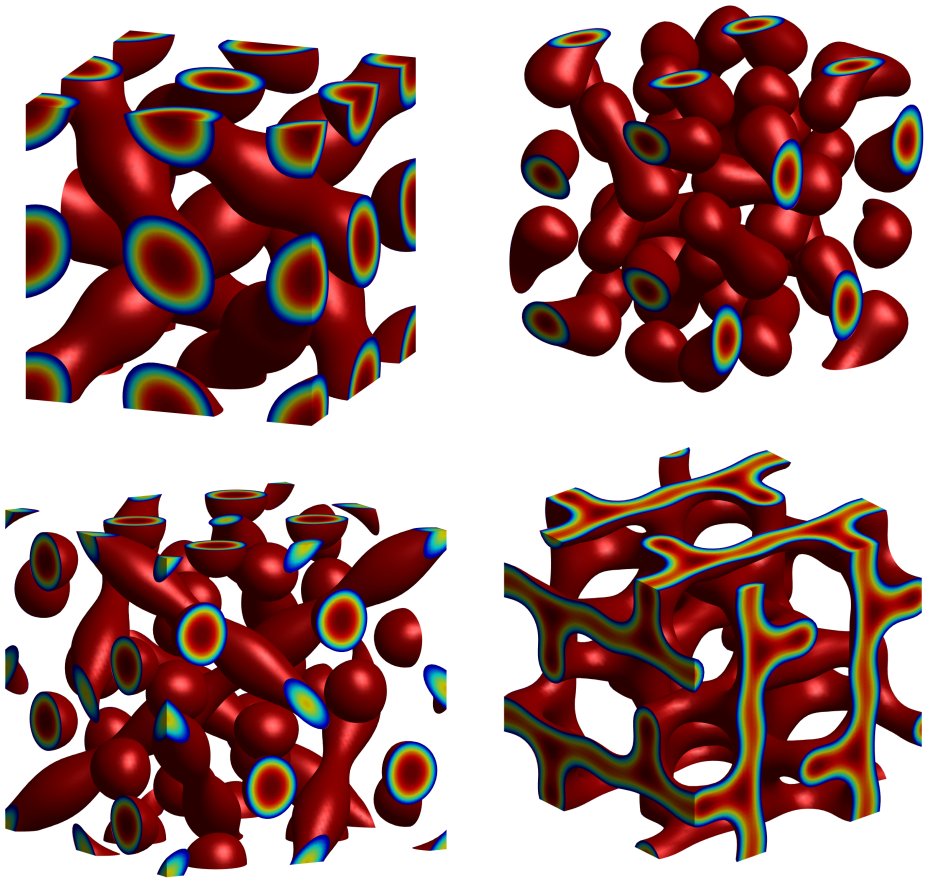

Figure 4.3: Exotic profiles from space group 230 computed at $m = 0.2, \gamma = 3$. Top: bumpy orthogonal cylinders ($l = 1.6, K = 35$) and lozenges ($l = 2.3, K = 35$). Bottom: mixed spheres and cylinders ($l = 2.3, K = 37$) and deformed double gyroids with right angle intersections ($l = 1.9, K = 27$). All profiles have been verified rigorously.

structures. This work is the first step towards rigorously computing the (minimal) energy landscape of the Ohta-Kawasaki functional in three dimensions. In future work we plan to extend this methodology to additional space groups and, once it is sufficiently efficient, use it to rigorously study the phase diagram of energy minimizing states, starting from the organizing center $m = 0, \gamma = 2$ and subsequently progressing to larger values of m and γ. To do this we need also to compute the energies with rigorous error bounds, work in general rectangular domains and optimize over the domain sizes. Any computation of the energy landscape also needs a method to verify local stability. We are hopeful that this can be dealt with naturally within the rigorous computational framework laid out in the current paper.

We have developed a novel method to enforce the physically observed symmetries in a computer-assisted proof setting. The algorithm works for general (symmetry) group actions in Fourier space, hence it is a natural next step to extend the applicability of this technique to other PDE problems with multiple symmetries.

Finally, some of the proofs require both patience and/or a considerable amount of memory. Only limited effort was made to optimize the code in these respects. Further work will include improving these performance measures. For example, calculating the nonlinear terms used an FFT of an array of size $N = 27(2K + 1)^3$. For $K = 50$ this leads to arrays of about 1GB in memory, growing about 5% per unit increase in K. This is a considerable problem as for small γ

solutions are very smooth but quickly approach the sharp front regime as γ increases. To resolve this we need larger values of K and the tails (in K) decay more slowly requiring even more modes. Reliably computing beyond $\gamma = 10$ would require approximately $K > 75$. Exploiting symmetry in the FFT algorithm is possible and could make the routine considerably more efficient (in memory and possibly runtime), but is beyond the scope of the current work.

Another avenue for refinement is to use different bounds in setting up the radii polynomial. It can be beneficial to use bounds which are slightly less sharp, and slightly more cumbersome to write down, but which can considerably reduce the computational effort (in particular for the bound Q_2). Although we did not pursue that here, mainly for expository reasons, we intend to include such algorithmic improvements in future efforts.

References

[1] F.S. Bates and G.H. Fredrickson. Block copolymer thermodynamics: Theory and experiment. *Annual Review of Physical Chemistry*, 41(1):525–557, 1990. PMID: 20462355.

[2] F.S. Bates and G.H. Fredrickson. Block copolymers - Designer soft materials. *Physics Today*, 52:32–38, 1999.

[3] R. Castelli, M. Gameiro, and J.-P. Lessard. Rigorous numerics for ill-posed PDEs: periodic orbits in the Boussinesq equation, 2017. To appear in Archive for Rational Mechanics and Analysis.

[4] R. Choksi, M. Maras, and J.F. Williams. 2D phase diagram for minimizers of a Cahn-Hilliard functional with long-range interactions. *SIAM J. Applied Dynamical Systems*, 10:1344–1362, 2011.

[5] R. Choksi and M.A. Peletier. Small volume fraction limit of the diblock copolymer problem: II. diffuse-interface functional. *SIAM J. Mathematical Analysis*, 43:739–763, 2011.

[6] R. Choksi, M.A. Peletier, and J.F. Williams. On the phase diagram for microphase separation of diblock copolymers: an approach via a nonlocal Cahn-Hilliard functional. *SIAM J. On Applied Mathematics*, 69:1712–1738, 2009.

[7] Eric W. Cochran, Carlos J. Garcia-Cervera, and Glenn H. Fredrickson. Stability of the gyroid phase in diblock copolymers at strong segregation. *Macromolecules*, 39(7):2449–2451, 2006.

[8] S. Day, J.-P. Lessard, and K. Mischaikow. Validated continuation for equilibria of PDEs. *SIAM J. Numerical Analysis*, 45:1398–1424, 2007.

[9] J.-L. Figueras and R. de la Llave. Numerical computations and computer assisted proofs of periodic orbits of the Kuramoto-Sivashinsky equation. *SIAM J. Appl. Dyn. Syst.*, 16(2):834–852, 2017.

[10] M. Gameiro and J.-P. Lessard. Analytic estimates and rigorous continuation for equilibria of higher-dimensional PDEs. *J. Differential Equations*, 249:2237–2268, 2010.

[11] M. Gameiro and J.-P. Lessard. A posteriori verification of invariant objects of evolution equations: periodic orbits in the Kuramoto-Sivashinsky PDE. *SIAM J. Appl. Dyn. Syst.*, 16(1):687–728, 2017.

[12] D. Goldman, C.B. Muratov, and S. Serfaty. The γ-limit of the two-dimensional Ohta–Kawasaki energy. Droplet arrangement via the renormalized energy. *Archive for Rational Mechanics and Analysis*, 212(2):445–501, May 2014.

[13] A. Hungria, J.-P. Lessard, and J.D. Mireles James. Rigorous numerics for analytic solutions of differential equations: the radii polynomial approach. *Mathematics of Computation*, 85:1427–1459, 2016.

[14] K. Hur and U. Wiesner. *Design and Applications of Multiscale Organic–Inorganic Hybrid Materials Derived from Block Copolymer Self-Assembly*, pages 259–293. Springer International Publishing, Cham, 2013.

[15] A.K. Khandpur, S. Forster, F.S. Bates, I.W. Hamley, A.J. Ryan, W. Bras, K. Almdal, and K. Mortensen. Polyisoprene-polystyrene diblock copolymer phase diagram near the order-disorder transition. *Macromolecules*, 28:8796–8806, 1995.

[16] J.-P. Lessard, E. Sander, and T. Wanner. Rigorous continuation of bifurcation points in the diblock copolymer equation, 2017. To appear in Journal of Computational Dynamics.

[17] T. Ohta and K. Kawasaki. Equilibrium morphology of block copolymer melts. *Macromolecules*, 19:2621–2632, 1986.

[18] S.M. Rump. INTLAB - INTerval LABoratory. In Tibor Csendes, editor, *Developments in Reliable Computing*, pages 77–104. Kluwer Academic Publishers, Dordrecht, 1999.

[19] S.M. Rump. Verification methods: Rigorous results using floating-point arithmetic. *Acta Numerica*, 19:287–449, 2010.

[20] D. Shirokoff, R. Choksi, and J.C. Nave. Sufficient conditions for global minimality of metastable states in a class of non-convex functionals: a simple approach via quadratic lower bounds. *J. of Nonlinear Science*, 25(3):539–582, 2015.

[21] T. Teramoto and Y. Nishiura. Double gyroid morphology in a gradient system with nonlocal effects. *Journal of the Physical Society of Japan*, 71(7):1611–1614, 2002.

[22] J.B. van den Berg. Introduction to rigorous numerics in dynamics: general functional analytic setup and an example that forces chaos, 2017. To appear in AMS Proceedings of Symposia in Applied Mathematics.

[23] J.B. van den Berg, M. Breden, J.-P. Lessard, and L. van Veen. Space-time periodic solutions of the Taylor-Green flow in the Navier-Stokes equations, 2017. In preparation.

[24] J.B. van den Berg and J.-P. Lessard. Chaotic braided solutions via rigorous numerics: chaos in the Swift-Hohenberg equation. *SIAM J. Applied Dynamical Systems*, 7:988–1031, 2008.

[25] J.B. van den Berg and J.-P. Lessard. Rigorous numerics in dynamics. *Notices Amer. Math. Soc.*, 62(9):1057–1061, 2015.

[26] J.B. van den Berg and J.F. Williams. The energy landscape of the Ohta-Kawasaki functional in three dimensions, 2017. In preparation.

[27] J.B. van den Berg and J.F. Williams. MATLAB code for "Rigorously computing symmetric stationary states of the Ohta-Kawasaki problem in 3D", 2017. `http://www.math.vu.nl/~janbouwe/code/OK3D/`.

[28] J.B. van den Berg and J.F. Williams. Validation of the bifurcation diagram in the 2D Ohta-Kawasaki problem. *Nonlinearity*, 30(4):1584, 2017.

[29] T. Wanner. Computer-assisted equilibrium validation for the diblock copolymer model. *Disc. and Cont. Dyn. Sys.*, 37(2):1075–1107, 2017.